Available online at www.sciencedirect.com
SCIENCE DIRECT®
International Journal of Solids and Structures 42 (2005) 971–1007
INTERNATIONAL JOURNAL OF SOLIDS and STRUCTURES
www.elsevier.com/locate/ijsolstr

A three-dimensional, higher-order, elasticity-based micromechanics model

Todd O. Williams *

Theoretical Division, T-3, Los Alamos National Laboratory, Los Alamos, NM 87545, USA

Received 1 April 2003; received in revised form 18 June 2004
Available online 3 September 2004

Abstract

The three-dimensional (3D) version of a new homogenization theory [A Two-Dimensional, Higher-Order, Elasticity-Based Micromechanics Model, in print] is presented. The 3D theory utilizes a higher-order, elasticity-based cell model (ECM) analysis for a periodic array of 3D unit cells. The unit cell is discretized into eight subregions or subcells. The displacement field within each subcell is approximated by a (truncated) eigenfunction expansion of up to fifth order. The governing equations are developed by satisfying the pointwise governing equations of geometrically linear continuum mechanics exactly up through the given order of the subcell displacement fields. The specified governing equations are valid for any type of constitutive model used to describe the behavior of the material in a subcell. The specialization of the theory to lower orders and to two-dimeinsions (2D) and to the exact one-dimensional (1D) theory is discussed.

Since the proposed 3D homogenization theory correctly reduces to both 2D and 1D the validation process applied to the 2D theory [A Two-Dimensional, Higher-Order, Elasticity-Based Micromechanics Model, in print] directly applies to the current formulation. Additional comparisons of the predicted responses obtained from the 3D ECM theory with existing published results are conducted. The good agreement obtained shows that the current theory represents a viable 3D homogenization tool. The improved agreement between the current theory results and published results as compared to the comparison of the MOC results and the published results is due to the correct incorporation of the coupling effects between the local fields. Additional results showing the convergence behavior of the average fields as a function of the order of the analysis is presented. These results show that the 1st order theory may not accurately predict the local averages but that consistent and converged behavior is obtained using the higher order ECM theories.

The proposed theory represents the necessary theoretical foundations for the development of exact homogenization solutions of generalized, three-dimensional microstructures.

* Tel.: +1 505 665 9190; fax: +1 505 665 5926.
E-mail address: oakhill@lanl.gov

0020-7683/$ - see front matter © 2004 Elsevier Ltd. All rights reserved.
doi:10.1016/j.ijsolstr.2004.06.056

Keywords: Micromechanics; Elasticity-based cell model (ECM); Particulate composites; Homogenization; Method of cells; Periodicity; Elasticity

1. Introduction

Most materials when viewed at the microstructural level, can be considered to have three-dimensional microstructures. Examples are polycrystalline metals, particulate composites, and high explosives. Three-dimensional (3D) homogenization based approaches are one method for modeling the effective behavior of such materials (Christensen, 1979; Aboudi, 1991; and Nemat-Nasser and Hori, 1993). Such models are capable of accounting directly for geometric effects within the microstructure, providing the concentration factors (Hill, 1963) that relate the local fields to the global fields, and predicting the material response under complex loading conditions. A particular homogenization approach which has proven highly successful is the 3D method of cells (MOC) analysis (Aboudi, 1991, 1996). One shortcoming of the 3D MOC theory is the lack of coupling between the local normal and shearing fields. This coupling between the different deformation phenomena is due to the presence of material property mismatches at the microstructural level as well as the geometric arrangement of the microstructure. The need for coupling the local fields is discussed more fully by Williams and Aboudi (1999).

Previous efforts, based more or less loosely on the original method of cells or generalized method of cells (GMC) analyzes (Paley and Aboudi, 1992), have been developed to address the need for coupled local effects in two-dimensional (2D) microstructures. The first effort by Williams and Aboudi (1999) carried out a weak solution analysis based on a general expansion for the displacement field within the subcells in a unit cell. A second theory was developed by Aboudi et al. (2001). This work also utilized a weak solution approach in conjunction with a partial, second order expansion for the displacement field in a subcell to analyze general microstructures. The above solution approaches are ''weak'' in the sense that both efforts apply a method of moments to the equilibrium equations approach in conjunction with integration by parts and the traction continuity equations to obtain the approximate governing equilibrium equations. Such an approach has been shown to be consistent with variational solution approaches, i.e. virtual work (Soldatos, 1995; Gilat, 1998) and thus the solution does not attempt to satisfy the pointwise governing equations. There are a number of considerations in the use of these approaches. In addition to the use of a weak formulation approach, the initial work by Williams and Aboudi (1999) introduced overly restrictive assumptions on the continuity behavior. The more recent weak solution approach pursued by Aboudi et al. (2001) has a number of differences from the original MOC/GMC type of analysis. First, while this approach has been formulated for complex microstructures it is not capable of analyzing the original microstructure associated with the MOC analysis due to the use of a second order expansion for the displacement field. Second, the approach is based on the use of the concepts of asymptotic homogenization (Bensoussan et al., 1978).

More recently, Williams (2004) has developed a elasticity based cell model (ECM) approach based on the use of eigenfunctions to describe the displacement field within a subcell which are part of a repeating unit cell. This work is based on a strong solution approach, i.e. on the solution of the pointwise governing equations of geometrically linear continuum mechanics as opposed to a variationally based solution approach. Consistent with the original MOC theory, this theory is based on the original microstructure proposed by Aboudi and provides all of the different concentration factors directly and simultaneously.

To date, no 3D analyzes equivalent to the above discussed 2D analyzes have been presented. The purpose of the current work is to extend the 2D analysis of Williams (2004) to three dimensions. In particular, the formulation for a new three-dimensional micromechanical theory utilizing an higher-order,

elasticity-based cell model (ECM) analysis is presented. The theory is based on the analysis of a triply periodic array of unit cells where each the unit cell is subdivided into eight subregions or subcells. The displacement field within each subcell is approximated by a (truncated) eigenfunction expansion of up to fifth order. The strong form of the pointwise governing equations of geometrically linear continuum mechanics are satisfied exactly up through an order consistent with the order of the subcell displacement fields. In particular, the formulation satisfies the equations of equilibrium within the subcells and the traction and displacement continuity constraints both between subcells and between unit cells. The theory is formulated independently of the material constitutive relations for the individual phases in the sense that the governing equations are appropriate for any type of (geometrically linear strain) constitutive theory. The third order theory is obtained through appropriate specialization of the fifth order theory. The specialization of the fifth and third order theories to the first order theory, which is equivalent to the MOC model given by Aboudi (1991), is discussed. The resulting 3D higher order theory correctly reduces to the equivalent higher order 2D theory for 2D microstructures as well as correctly reducing to the exact solution for a bilaminated material (Aboudi, 1991). It is shown that both of the current 3D formulations can accurately predict the bulk elastic properties of both continuous fiber and particulate composites as well as the associated local fields. Additionally, the convergence behavior of the average fields predicted by the different orders of the ECM theory are examined. It is shown that while the first order theory may not accurately predict the local behavior, using the higher order ECM theories results in consistent and converged predictions. The primary focus of the current paper is on the fundamental formulation of the 3D theory. For this purpose it is sufficient to consider only elastic behavior. The extension of the theory to inelastic analysis is outlined in brief. This extension will be addressed more fully in future work.

It is useful to put the proposed theory in perspective with respect to other types of micromechanical analyzes. While average field theories (such as those based on Eshelby's analysis (1957) e.g. the Mori-Tanaka theory (Benveniste, 1987)) can adequately predict the effective elastic behavior of heterogeneous materials these types of theories are not capable of accurately predicting the effective inelastic behavior of such materials due to their inability to predict fluctuating fields about the phase average responses within the microstructure. In order to correctly predict these fluctuating responses, which drive the initiation and evolution of history-dependent behavior (see for example Williams and Pindera, 1997), it is necessary to employ homogenization theories capable of predicting spatially varying field effects within each phase. Some simplified theories (frequently referred to as cell models) attempt to obtain more accurate representations of the local fields by selectively employing isostrain and/or isostress assumptions in localized subregions. These types of approaches do not, in general, correctly satisfy all of the governing equations of continuum mechanics or exhibit coupling of the local shear and normal fields (which is one of the major issues addressed within the current theory). In order to obtain accurate estimates of the local fluctuating fields, and, hence, of the global inelastic response, it is necessary to consider substantially more sophisticated theories. These approaches can be roughly separated into two different classes. The first class of approaches are analytical and are based on satisfying the governing equations of continuum mechanics in a strong sense, i.e. solving these equations in a pointwise fashion. Examples of such types of approaches are elasticity based solutions (see for example Williams and Pindera, 1995, 1997) or Green's function based analyzes (see Walker et al., 1993 or Nemat-Nasser and Hori, 1993). The second class of approaches are numerical in nature. In general, this class of techniques satisfies the governing equations in a weak (variational) sense. Examples of these types of techniques are finite element based analyzes (both conventional and periodic). Both classes of techniques represent viable approaches to analyzing the response of heterogeneous materials with each class having different strengths and weaknesses. The proposed theory falls within the first class.

The proposed theory has a number of strengths and weaknesses when compared to other theories in the two different classes mentioned above. In general, analytical theories have a number of advantages over numerical approaches. These types of theories can be used to study local interaction effects in the

microstructure that are not necessarily easily considered within the context of FE analyzes. Second, the first class of theories provide analytical expressions for all of the mechanical and eigenstrain concentration tensors directly and simultaneously. Alternatively, the evaluation of the concentration tensors using numerical approaches requires a sequencial application of the numerical analysis; one for each potential loading state, which in the case of history-dependent behavior can involve substantial computational cost. Third, analytical approaches can be used to study functional relations within the concentration tensors and, hence, the influence different aspects of the microstructure or the phase properties have on the local and bulk material response. Finally, due to their ability to generate the concentration tensors in analytical form and simultaneously, analytical models can be used to study functional forms for the bulk constitutive relations while this process is substantially more difficult within the context of FE based analyzes. Since the proposed approach falls within the first class of analyzes it has all of the above outlined advantages.

Numerical approaches have important strengths in their abilities to deal with complex microstructures subjected to complex loading states. Many analytical models do not have these capabilities and are specialized to the analysis of certain types of bulk loading or to specfic microstructural geometries (see Williams and Pindera, 1995, 1997 for example). While the current variant of the proposed theory is limited to the analysis of rather specialized microstructures, the approach forms the cornerstone for the development of exact elasticity based analyzes for arbitrary microstructures based on infinite series solutions (developed in future work). The development of this cornerstone represents one of the most important contributions of the proposed theory. From a practical point of view the proposed solutions given in the following development represent the lowest order, truncated solutions in the infinite series solution that correctly couple the local fields. It is noted that when applicable exact solutions are obviously highly desirable.

The current theory has a number of other capabilities that should be recognized. The current model is sufficiently computationally efficient (in terms of the number of basic unknowns) that it can be implemented into structural analysis codes as a material constitutive model. The author's experience has shown the current approach to be more computationally efficient than some other elasticity based analyzes such as the concentric cylinders model for inelastic behavior (Williams and Pindera, 1995, 1997). The proposed theory's computationally efficiency can be significantly enhanced (by a reduction in the number of unknowns of almost 50%) by reformulating the governing equations using the local-global stiffness matrix (LGSM) approach (Williams and Pindera, 1995, 1997). The application of the LGSM reformulation to the proposed theory will be carried out in future work. Furthermore, an alternative to implementing the full form of the proposed theory into structural analysis codes can be developed by utilizing the theory's ability to generate increasingly more accurate estimates for local piecewise uniform fields without the need to solve for the higher order terms in the theory (addressed in future work). Following this approach results in a substantial reduction in the number of unknowns with a corresponding increase in computational efficiency. The use of local piecewise uniform fields as the basis for estimates for the bulk material behavior is a common practice in the implementation of homogenization concepts into structural analysis codes. Finally, the proposed theory can be employed in a sequential fashion by switching from lower order analyzes to higher order analyzes (and vice versa) on the fly. This last capability has obvious implications for both accuracy and computation efficiency as well as being the basis for considering convergence behavior as loading progresses for inelastic analyzes.

2. Theoretical framework for a fifth order theory

The development of the 3D theory directly parallels that of the 2D formulation (Williams, 2004). The following conventions are used throughout the formulation. Summation is implied on Latin alphabetic

and Arabic numeric subscripts and superscripts. An overbar denotes a mean (volume averaged) field. For some generic field f this mean field is related to the pointwise field by

$$\bar{f} = \frac{1}{V}\int f \, \mathrm{d}V$$

where V is the volume of the unit cell. The associated fluctuating field is given by

$$f' = f - \bar{f}$$

The fluctuating field has a zero mean ($\overline{f'} = 0$).

Various field expansions are utilized in the following formulation. The quantities on the left hand side of these equations, $u_i^{(\alpha,\beta,\gamma)}$ in Eq. (2.2), $\epsilon_{ij}^{(\alpha,\beta,\gamma)}$ in Eq. (2.3), and $\sigma_{ij}^{(\alpha,\beta,\gamma)}$ in Eq. (2.4), denote the pointwise value of the field within the (α, β, γ) subcell, Fig. 1. The different constants in these field expansions (which occur on the left hand side of these equations) are denoted by the $V_{i(m,n,r)}^{(\alpha,\beta,\gamma)}$ in Eq. (2.2), the $\mu_{ij(p,q,s)}^{(\alpha,\beta,\gamma)}$ in Eq. (2.3), and $\sigma_{ij(p,q,s)}^{(\alpha,\beta,\gamma)}$ in Eq. (2.4). The subscripts (m, n, r) or (p, q, s) denote the order of the constant, i.e. the associated order of the expansion functions. The superscripts (α,β,γ) denote the associated subcell (in the unit cell) in which the field expansion exists where α, β, and γ range from 1 to 2 individually. When feasible the superscripts α, β, and γ are dropped and in these cases it is to be understood that the associated discussion applies to all subcells. A local coordinate system $\bar{x}_i$ is defined at the center of each subcell.

2.1. Subcell fields

Consider a triply periodic array of inclusions embedded in a matrix (Fig. 1). The composite system is subjected to the displacement field

$$U_i = \overline{\epsilon}_{ij} x_j \tag{2.1}$$

where the $\overline{\epsilon}_{ij}$ are the bulk (average) strains in the composite and the x_j are the macroscopic coordinates in the composite.

Implied by this type of material microstructure and global loading state is the fact that it is sufficient to analyze only a *single* repeating unit cell (Fig. 1). In particular, the proposed microstructure and bulk loading state implies that the local fields are periodic and, hence, all unit cells behave the same with respect to the stresses and strains. As originally proposed by Aboudi (1991) this unit cell is subdivided into eight subregions or subcells. Each subcell is considered to be occupied by a single material. In general, at least one of the subcells will be occupied by the material which is considered to be the inclusion phase with the remaining subcells occupied by the matrix material. Note that if all of the subcells are occupied by the same material then the material is a homogeneous material and the proposed theory predicts that all fluctuating field effects are identically zero as required.

The assumed subcell displacement field is

$$u_i^{(\alpha,\beta,\gamma)} = \overline{\epsilon}_{ij} x_j + P_{(m,n,r)} V_{i(m,n,r)}^{(\alpha,\beta,\gamma)} \tag{2.2}$$

where

$$P_{(m,n,r)} = p_m(\bar{x}_1) p_n(\bar{x}_2) p_r(\bar{x}_3)$$

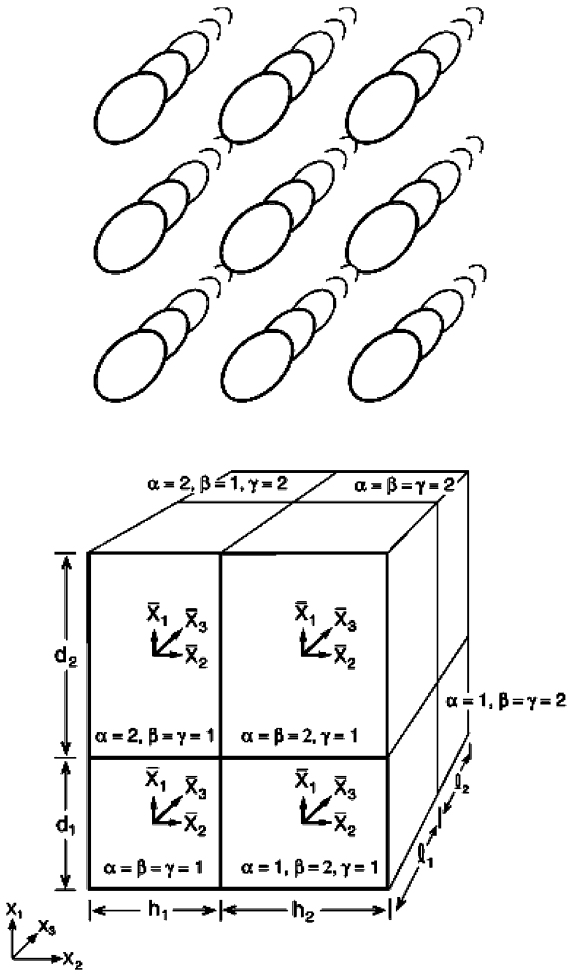

Fig. 1. The discretized unit cell for a particulate composite used by both the original MOC model and the ECM.

and the $p_m(\bar{x}_1)$, $p_n(\bar{x}_2)$, $p_r(\bar{x}_3)$ are dimensional Legendre polynomials of order m in $\bar{x}_1$, n in $\bar{x}_2$, and r in $\bar{x}_3$, respectively, the $\bar{x}_i$ represent the local coordinates in the subcell, the m, n, and r range from 1 to 5 individually, and the cumulative order, denoted by $m+n+r$ must be an odd number (i.e. 1, 3, or 5). The particular forms for the dimensional Legendre polynomials are given in Appendix A. As mentioned above, summation is assumed on the subscripts m, n, and r. The $V^{(\alpha,\beta,\gamma)}_{i(m,n,r)}$ are constants that represent the material microstructure induced fluctuating displacement field effects about the applied displacement field, Eq. (2.1). There are 102 unknown $V^{(\alpha,\beta,\gamma)}_{i(m,n,r)}$ per subcell which gives 816 unknowns per unit cell. As was the situation in the 2D theory (Williams, 2004) the even cumulative order terms are not considered since they decouple from the odd cumulative order and hence are identically zero. Eq. (2.2) is written out in expanded form in the Appendix A.

Using the geometrically linear strain-displacement relations

$$\epsilon_{ij} = \frac{1}{2}(\partial_j u_i + \partial_i u_j)$$

the strains within a given subcell have the following functional form

$$\epsilon_{ij}^{(\alpha,\beta,\gamma)} = P_{(p,q,s)}\epsilon_{ij(p,q,s)}^{(\alpha,\beta,\gamma)} = P_{(0,0,0)}\bar{\epsilon}_{ij} + P_{(p,q,s)}\mu_{ij(p,q,s)}^{(\alpha,\beta,\gamma)} \tag{2.3}$$

where p, q, and s range from 0 to 4 individually and the cumulative order, $p+q+s$, must be an even number (i.e. 0, 2, or 4). The fact that the cumulative order, $p+q+s$, for the strains must be an even number is consistent with the fact that only odd cumulative order ($m+n+r$) terms exist in the displacement expansion, Eq. (2.2), which upon differentiation lead to strains of even cumulative order $p+q+s$. The $\mu_{ij(p,q,s)}^{(\alpha,\beta,\gamma)}$ represent fluctuating strain effects. These terms are defined in Appendix A. The expanded version of Eq. (2.3) is given in Appendix A.

The corresponding stress field is

$$\sigma_{ij}^{(\alpha,\beta,\gamma)} = P_{(p,q,s)}\sigma_{ij(p,q,s)}^{(\alpha,\beta,\gamma)} \tag{2.4}$$

where $\sigma_{ij(p,q,s)}^{(\alpha,\beta,\gamma)}$ are the stress terms associated with the expansion function $P_{(p,q,s)}$ in the different subcells. The expanded version of Eq. (2.4) is given in Appendix A.

The following formulation is carried out independently of any particular set of constitutive relations and, hence, the basic theory places no restrictions on the constitutive equations that relate the strain field, Eq. (2.3), and the stress field, Eq. (2.4). However, to solve for the fundamental unknowns in the theory, the $V_{i(m,n,r)}^{(\alpha,\beta,\gamma)}$, it is ultimately necessary to specify particular constitutive relations. Specification of a particular set of such relations allows the stresses to be directly written in terms of the kinematic unknowns $V_{i(m,n,r)}^{(\alpha,\beta,\gamma)}$ (and appropriate history-dependent effects such as plastic strains for example). In the case of linear elastic constituents the following constitutive relations can be obtained

$$\sigma_{ij(p,q,s)}^{(\alpha,\beta,\gamma)} = C_{ijkl}^{(\alpha,\beta,\gamma)}\epsilon_{kl(p,q,s)}^{(\alpha,\beta,\gamma)}$$

where the $C_{ijkl}^{(\alpha,\beta,\gamma)}$ are the components of the stiffness tensor in a subcell. Using the expressions for the strain terms $\mu_{ij(p,q,s)}^{(\alpha,\beta,\gamma)}$ (given in Appendix A) the stress terms $\sigma_{ij(p,q,s)}^{(\beta,\gamma)}$ can be directly expressed as functions of the fundamental unknowns, the $V_{i(m,n,r)}^{(\alpha,\beta,\gamma)}$. The resulting relations can be subsequently substituted into the governing equations developed in the following formuation in order to express these equations solely in terms of the kinematic unknowns. If the more general form for the Hookean relations given by

$$\sigma_{ij} = C_{ijkl}\epsilon_{kl} + \lambda_{ij}$$

where the λ_{ij} represent eigenstress effects, is assumed then the particulars of the constitutive relations obviously change but the basic procedure for expressing the governing equations in terms of the kinematic unknowns remains unchanged. It is noted that a broad variety of constitutive relations, such as viscoelastic, plastic, and viscoplastic constitutive theories can be cast in the above form. For example, in a plasticity theory based on superposition of strain effects, the eigenstress is given by $\lambda_{ij} = -C_{ijkl}\epsilon_{kl}^{P}$ where ϵ_{kl}^{P} are the plastic strains. The use of the above form for the constitutive relations does not preclude the necessity of incrementally evaluating the evolution of the internal state variables associated with the history-dependence.

2.2. Governing equations for fifth order theory

The strong (pointwise) form of the equilibrium equations are given by

$$\partial_1\sigma_{i1} + \partial_2\sigma_{i2} + \partial_3\sigma_{i3} = 0$$

Substituting the subcell stress field, Eq. (2.4), into the above relation, collecting terms of the same order, and setting each grouping to zero gives a system of governing equilibrium equations for a subcell. This process is equivalent to using the orthogonality properties of the eigenfunctions (see Williams (2004) for equivalent details). These governing equations satisfy the strong form exactly up to an order consistent with the order of approximation of the subcell fields. The first order equilibrium equations for a subcell are

$$3\sigma_{i1(200)}^{(\alpha,\beta,\gamma)}+\sigma_{i2(110)}^{(\alpha,\beta,\gamma)}+\sigma_{i3(101)}^{(\alpha,\beta,\gamma)}+\left(\frac{d_\alpha}{2}\right)^2\sigma_{i1(400)}^{(\alpha,\beta,\gamma)}+\left(\frac{h_\beta}{2}\right)^2\sigma_{i2(130)}^{(\alpha,\beta,\gamma)}+\left(\frac{l_\gamma}{2}\right)^2\sigma_{i3(103)}^{(\alpha,\beta,\gamma)}=0 \tag{2.5}$$

$$\sigma_{i1(110)}^{(\alpha,\beta,\gamma)}+3\sigma_{i2(020)}^{(\alpha,\beta,\gamma)}+\sigma_{i3(011)}^{(\alpha,\beta,\gamma)}+\left(\frac{d_\alpha}{2}\right)^2\sigma_{i1(310)}^{(\alpha,\beta,\gamma)}+3\left(\frac{h_\beta}{2}\right)^2\sigma_{i2(040)}^{(\alpha,\beta,\gamma)}+\left(\frac{l_\gamma}{2}\right)^2\sigma_{i3(013)}^{(\alpha,\beta,\gamma)}=0 \tag{2.6}$$

$$\sigma_{i1(101)}^{(\alpha,\beta,\gamma)}+\sigma_{i2(011)}^{(\alpha,\beta,\gamma)}+3\sigma_{i3(002)}^{(\alpha,\beta,\gamma)}+\left(\frac{d_\alpha}{2}\right)^2\sigma_{i1(301)}^{(\alpha,\beta,\gamma)}+\left(\frac{h_\beta}{2}\right)^2\sigma_{i2(031)}^{(\alpha,\beta,\gamma)}+3\left(\frac{l_\gamma}{2}\right)^2\sigma_{i3(004)}^{(\alpha,\beta,\gamma)}=0 \tag{2.7}$$

where d_α, h_β, and l_γ denote the lengths of the sides along the x_1, x_2, and x_3 directions of the (α,β,γ) subcell (see Fig. 1). The corresponding third order equilibrium equations are

$$\sigma_{i1(103)}^{(\alpha,\beta,\gamma)}+\sigma_{i2(013)}^{(\alpha,\beta,\gamma)}+7\sigma_{i3(004)}^{(\alpha,\beta,\gamma)}=0 \tag{2.8}$$

$$\sigma_{i1(112)}^{(\alpha,\beta,\gamma)}+3\sigma_{i2(022)}^{(\alpha,\beta,\gamma)}+5\sigma_{i3(013)}^{(\alpha,\beta,\gamma)}=0 \tag{2.9}$$

$$\sigma_{i1(121)}^{(\alpha,\beta,\gamma)}+5\sigma_{i2(031)}^{(\alpha,\beta,\gamma)}+3\sigma_{i3(022)}^{(\alpha,\beta,\gamma)}=0 \tag{2.10}$$

$$\sigma_{i1(130)}^{(\alpha,\beta,\gamma)}+7\sigma_{i2(040)}^{(\alpha,\beta,\gamma)}+\sigma_{i3(031)}^{(\alpha,\beta,\gamma)}=0 \tag{2.11}$$

$$3\sigma_{i1(202)}^{(\alpha,\beta,\gamma)}+\sigma_{i2(112)}^{(\alpha,\beta,\gamma)}+5\sigma_{i3(103)}^{(\alpha,\beta,\gamma)}=0 \tag{2.12}$$

$$3\sigma_{i1(211)}^{(\alpha,\beta,\gamma)}+3\sigma_{i2(121)}^{(\alpha,\beta,\gamma)}+3\sigma_{i3(112)}^{(\alpha,\beta,\gamma)}=0 \tag{2.13}$$

$$3\sigma_{i1(220)}^{(\alpha,\beta,\gamma)}+5\sigma_{i2(130)}^{(\alpha,\beta,\gamma)}+\sigma_{i3(121)}^{(\alpha,\beta,\gamma)}=0 \tag{2.14}$$

$$5\sigma_{i1(301)}^{(\alpha,\beta,\gamma)}+\sigma_{i2(211)}^{(\alpha,\beta,\gamma)}+3\sigma_{i3(202)}^{(\alpha,\beta,\gamma)}=0 \tag{2.15}$$

$$5\sigma_{i1(310)}^{(\alpha,\beta,\gamma)}+3\sigma_{i2(220)}^{(\alpha,\beta,\gamma)}+\sigma_{i3(211)}^{(\alpha,\beta,\gamma)}=0 \tag{2.16}$$

$$7\sigma_{i1(400)}^{(\alpha,\beta,\gamma)}+\sigma_{i2(310)}^{(\alpha,\beta,\gamma)}+\sigma_{i3(301)}^{(\alpha,\beta,\gamma)}=0 \tag{2.17}$$

There are 9 first order and 30 third order equilibrium equations per subcell. Thus, the above system of equilibrium equations represent 312 governing equations. Note that the fact that the above equilibrium equations are of odd cumulative order is due to the fact that they are based directly on the pointwise form of the equilibrium equations which require spatial differentiation of the stress field. If even cumulative order terms had been included in the analysis they would not have entered into the above equations but instead would have generated additional (zero and second cumulative order) governing equilibrium equations.

Next the displacement continuity equations across interfaces are developed. These continuity equations are obtained by substituting Eq. (2.2) into the pointwise form of the displacement continuity constraints

$$u_i^+ = u_i^-$$

collecting terms with the same spatial variation characteristics, and setting each grouping to zero (see Williams (2004) for equivalent details). Note that the superscripts $\pm$ in the above relation are used to denote the different sides of an interface. The displacement continuity conditions are imposed through a cumulative order of two across each interface (which is consistent with the 2D theory). For faces with the normal in the x_1 direction the appropriate continuity equations are

$$\frac{d_1}{2}V_{i(100)}^{(1,\beta,\gamma)} + \left(\frac{d_1}{2}\right)^3 V_{i(300)}^{(1,\beta,\gamma)} + \left(\frac{d_1}{2}\right)^5 V_{i(500)}^{(1,\beta,\gamma)} = -\frac{d_2}{2}V_{i(100)}^{(2,\beta,\gamma)} - \left(\frac{d_2}{2}\right)^3 V_{i(300)}^{(2,\beta,\gamma)} - \left(\frac{d_2}{2}\right)^5 V_{i(500)}^{(2,\beta,\gamma)} \tag{2.18}$$

$$V_{i(010)}^{(1,\beta,\gamma)} + \left(\frac{d_1}{2}\right)^2 V_{i(210)}^{(1,\beta,\gamma)} + \left(\frac{d_1}{2}\right)^4 V_{i(410)}^{(1,\beta,\gamma)} = V_{i(010)}^{(2,\beta,\gamma)} + \left(\frac{d_2}{2}\right)^2 V_{i(210)}^{(2,\beta,\gamma)} + \left(\frac{d_2}{2}\right)^4 V_{i(410)}^{(2,\beta,\gamma)} \tag{2.19}$$

$$V_{i(001)}^{(1,\beta,\gamma)} + \left(\frac{d_1}{2}\right)^2 V_{i(201)}^{(1,\beta,\gamma)} + \left(\frac{d_1}{2}\right)^4 V_{i(401)}^{(1,\beta,\gamma)} = V_{i(001)}^{(2,\beta,\gamma)} + \left(\frac{d_2}{2}\right)^2 V_{i(201)}^{(2,\beta,\gamma)} + \left(\frac{d_2}{2}\right)^4 V_{i(401)}^{(2,\beta,\gamma)} \tag{2.20}$$

$$\frac{d_1}{2}V_{i(111)}^{(1,\beta,\gamma)} + \left(\frac{d_1}{2}\right)^3 V_{i(311)}^{(1,\beta,\gamma)} = -\frac{d_2}{2}V_{i(111)}^{(2,\beta,\gamma)} - \left(\frac{d_2}{2}\right)^3 V_{i(311)}^{(2,\beta,\gamma)} \tag{2.21}$$

$$\frac{d_1}{2}V_{i(120)}^{(1,\beta,\gamma)} + \left(\frac{d_1}{2}\right)^3 V_{i(320)}^{(1,\beta,\gamma)} = -\frac{d_2}{2}V_{i(120)}^{(2,\beta,\gamma)} - \left(\frac{d_2}{2}\right)^3 V_{i(320)}^{(2,\beta,\gamma)} \tag{2.22}$$

$$\frac{d_1}{2}V_{i(102)}^{(1,\beta,\gamma)} + \left(\frac{d_1}{2}\right)^3 V_{i(302)}^{(1,\beta,\gamma)} = -\frac{d_2}{2}V_{i(102)}^{(2,\beta,\gamma)} - \left(\frac{d_2}{2}\right)^3 V_{i(302)}^{(2,\beta,\gamma)} \tag{2.23}$$

For faces with the normal in the x_2 direction the appropriate continuity equations are

$$\frac{h_1}{2}V_{i(010)}^{(\alpha,1,\gamma)} + \left(\frac{h_1}{2}\right)^3 V_{i(030)}^{(\alpha,1,\gamma)} + \left(\frac{h_1}{2}\right)^5 V_{i(050)}^{(\alpha,1,\gamma)} = -\frac{h_2}{2}V_{i(010)}^{(\alpha,2,\gamma)} - \left(\frac{h_2}{2}\right)^3 V_{i(030)}^{(\alpha,2,\gamma)} - \left(\frac{h_2}{2}\right)^5 V_{i(050)}^{(\alpha,2,\gamma)} \tag{2.24}$$

$$V_{i(100)}^{(\alpha,1,\gamma)} + \left(\frac{h_1}{2}\right)^2 V_{i(120)}^{(\alpha,1,\gamma)} + \left(\frac{h_1}{2}\right)^4 V_{i(140)}^{(\alpha,1,\gamma)} = V_{i(100)}^{(\alpha,2,\gamma)} + \left(\frac{h_2}{2}\right)^2 V_{i(120)}^{(\alpha,2,\gamma)} + \left(\frac{h_2}{2}\right)^4 V_{i(140)}^{(\alpha,2,\gamma)} \tag{2.25}$$

$$V_{i(001)}^{(\alpha,1,\gamma)} + \left(\frac{h_1}{2}\right)^2 V_{i(021)}^{(\alpha,1,\gamma)} + \left(\frac{h_1}{2}\right)^4 V_{i(041)}^{(\alpha,1,\gamma)} = V_{i(001)}^{(\alpha,2,\gamma)} + \left(\frac{h_2}{2}\right)^2 V_{i(021)}^{(\alpha,2,\gamma)} + \left(\frac{h_2}{2}\right)^4 V_{i(041)}^{(\alpha,2,\gamma)} \tag{2.26}$$

$$\frac{h_1}{2}V_{i(111)}^{(\alpha,1,\gamma)} + \left(\frac{h_1}{2}\right)^3 V_{i(131)}^{(\alpha,1,\gamma)} = -\frac{h_2}{2}V_{i(111)}^{(\alpha,2,\gamma)} - \left(\frac{h_2}{2}\right)^3 V_{i(131)}^{(\alpha,2,\gamma)} \tag{2.27}$$

$$\frac{h_1}{2}V_{i(210)}^{(\alpha,1,\gamma)} + \left(\frac{h_1}{2}\right)^3 V_{i(230)}^{(\alpha,1,\gamma)} = -\frac{h_2}{2}V_{i(210)}^{(\alpha,2,\gamma)} - \left(\frac{h_2}{2}\right)^3 V_{i(230)}^{(\alpha,2,\gamma)} \tag{2.28}$$

$$\frac{h_1}{2}V_{i(012)}^{(\alpha,1,\gamma)} + \left(\frac{h_1}{2}\right)^3 V_{i(032)}^{(\alpha,1,\gamma)} = -\frac{h_2}{2}V_{i(012)}^{(\alpha,2,\gamma)} - \left(\frac{h_2}{2}\right)^3 V_{i(032)}^{(\alpha,2,\gamma)} \tag{2.29}$$

For faces with the normal in the x_3 direction the appropriate continuity equations are

$$\frac{l_1}{2}V^{(\alpha,\beta,1)}_{i(001)} + \left(\frac{l_1}{2}\right)^3 V^{(\alpha,\beta,1)}_{i(003)} + \left(\frac{l_1}{2}\right)^5 V^{(\alpha,\beta,1)}_{i(005)} = -\frac{l_2}{2}V^{(\alpha,\beta,2)}_{i(001)} - \left(\frac{l_2}{2}\right)^3 V^{(\alpha,\beta,2)}_{i(003)} - \left(\frac{l_2}{2}\right)^5 V^{(\alpha,\beta,2)}_{i(005)} \tag{2.30}$$

$$V^{(\alpha,\beta,1)}_{i(100)} + \left(\frac{l_1}{2}\right)^2 V^{(\alpha,\beta,1)}_{i(102)} + \left(\frac{l_1}{2}\right)^4 V^{(\alpha,\beta,1)}_{i(104)} = V^{(\alpha,\beta,2)}_{i(100)} + \left(\frac{l_2}{2}\right)^2 V^{(\alpha,\beta,2)}_{i(102)} + \left(\frac{l_2}{2}\right)^4 V^{(\alpha,\beta,2)}_{i(104)} \tag{2.31}$$

$$V^{(\alpha,\beta,1)}_{i(010)} + \left(\frac{l_1}{2}\right)^2 V^{(\alpha,\beta,1)}_{i(012)} + \left(\frac{l_1}{2}\right)^4 V^{(\alpha,\beta,1)}_{i(014)} = V^{(\alpha,\beta,2)}_{i(010)} + \left(\frac{l_2}{2}\right)^2 V^{(\alpha,\beta,2)}_{i(012)} + \left(\frac{l_2}{2}\right)^4 V^{(\alpha,\beta,2)}_{i(014)} \tag{2.32}$$

$$\frac{l_1}{2}V^{(\alpha,\beta,1)}_{i(111)} + \left(\frac{l_1}{2}\right)^3 V^{(\alpha,\beta,1)}_{i(113)} = -\frac{l_2}{2}V^{(\alpha,\beta,2)}_{i(111)} - \left(\frac{l_2}{2}\right)^3 V^{(\alpha,\beta,2)}_{i(113)} \tag{2.33}$$

$$\frac{l_1}{2}V^{(\alpha,\beta,1)}_{i(201)} + \left(\frac{l_1}{2}\right)^3 V^{(\alpha,\beta,1)}_{i(203)} = -\frac{l_2}{2}V^{(\alpha,\beta,2)}_{i(201)} - \left(\frac{l_2}{2}\right)^3 V^{(\alpha,\beta,2)}_{i(203)} \tag{2.34}$$

$$\frac{l_1}{2}V^{(\alpha,\beta,1)}_{i(021)} + \left(\frac{l_1}{2}\right)^3 V^{(\alpha,\beta,1)}_{i(023)} = -\frac{l_2}{2}V^{(\alpha,\beta,2)}_{i(021)} - \left(\frac{l_2}{2}\right)^3 V^{(\alpha,\beta,2)}_{i(023)} \tag{2.35}$$

There are 12 zeroth order, 24 first order, and 36 second order displacement continuity equations in each direction resulting in a total of 216 governing displacement continuity relations for the unit cell. Note that the above forms of the displacement continuity equations account for both the continuity between subcells as well as the continuity conditions between unit cells, i.e. these equations explicitly satisfy all of the periodicity constraints in the problem.

The next step in the formulation is the development of the governing traction continuity equations. The pointwise forms of these constraints are

$$t_i^+ = -t_i^-$$

The appropriate traction continuity equations are determined by substituting Eq. (2.4) into the above relation, collecting terms with the same spatial dependency, and setting each grouping to zero. In order to be consistent with the displacement continuity equations, this process must also be carried out through a cumulative order of two. For faces with the normal in the x_1 direction the traction continuity equations are

$$\sigma^{(1,\beta,\gamma)}_{i1(000)} + \left(\frac{d_1}{2}\right)^2 \sigma^{(1,\beta,\gamma)}_{i1(200)} + \left(\frac{d_1}{2}\right)^4 \sigma^{(1,\beta,\gamma)}_{i1(400)} = \sigma^{(2,\beta,\gamma)}_{i1(000)} + \left(\frac{d_2}{2}\right)^2 \sigma^{(2,\beta,\gamma)}_{i1(200)} + \left(\frac{d_2}{2}\right)^4 \sigma^{(2,\beta,\gamma)}_{i1(400)} \tag{2.36}$$

$$\frac{d_1}{2}\sigma^{(1,\beta,\gamma)}_{i1(110)} + \left(\frac{d_1}{2}\right)^3 \sigma^{(1,\beta,\gamma)}_{i1(310)} = -\frac{d_2}{2}\sigma^{(2,\beta,\gamma)}_{i1(110)} - \left(\frac{d_2}{2}\right)^3 \sigma^{(2,\beta,\gamma)}_{i1(310)} \tag{2.37}$$

$$\frac{d_1}{2}\sigma^{(1,\beta,\gamma)}_{i1(101)} + \left(\frac{d_1}{2}\right)^3 \sigma^{(1,\beta,\gamma)}_{i1(301)} = -\frac{d_2}{2}\sigma^{(2,\beta,\gamma)}_{i1(101)} - \left(\frac{d_2}{2}\right)^3 \sigma^{(2,\beta,\gamma)}_{i1(301)} \tag{2.38}$$

$$\sigma^{(1,\beta,\gamma)}_{i1(011)} + \left(\frac{d_1}{2}\right)^2 \sigma^{(1,\beta,\gamma)}_{i1(211)} = \sigma^{(2,\beta,\gamma)}_{i1(011)} + \left(\frac{d_2}{2}\right)^2 \sigma^{(2,\beta,\gamma)}_{i1(211)} \tag{2.39}$$

$$\sigma_{i1(020)}^{(1,\beta,\gamma)} + \left(\frac{d_1}{2}\right)^2 \sigma_{i1(220)}^{(1,\beta,\gamma)} = \sigma_{i1(020)}^{(2,\beta,\gamma)} + \left(\frac{d_2}{2}\right)^2 \sigma_{i1(220)}^{(2,\beta,\gamma)} \tag{2.40}$$

$$\sigma_{i1(002)}^{(1,\beta,\gamma)} + \left(\frac{d_1}{2}\right)^2 \sigma_{i1(202)}^{(1,\beta,\gamma)} = \sigma_{i1(002)}^{(2,\beta,\gamma)} + \left(\frac{d_2}{2}\right)^2 \sigma_{i1(202)}^{(2,\beta,\gamma)} \tag{2.41}$$

For faces with the normal in the x_2 direction the traction continuity equations are

$$\sigma_{i2(000)}^{(\alpha,1,\gamma)} + \left(\frac{h_1}{2}\right)^2 \sigma_{i2(020)}^{(\alpha,1,\gamma)} + \left(\frac{h_1}{2}\right)^4 \sigma_{i2(040)}^{(\alpha,1,\gamma)} = \sigma_{i2(000)}^{(\alpha,2,\gamma)} + \left(\frac{h_2}{2}\right)^2 \sigma_{i2(020)}^{(\alpha,2,\gamma)} + \left(\frac{h_2}{2}\right)^4 \sigma_{i2(040)}^{(\alpha,2,\gamma)} \tag{2.42}$$

$$\frac{h_1}{2}\sigma_{i2(110)}^{(\alpha,1,\gamma)} + \left(\frac{h_1}{2}\right)^3 \sigma_{i2(130)}^{(\alpha,1,\gamma)} = -\frac{h_2}{2}\sigma_{i2(110)}^{(\alpha,2,\gamma)} - \left(\frac{h_2}{2}\right)^3 \sigma_{i2(13)}^{(\alpha,2,\gamma)} \tag{2.43}$$

$$\frac{h_1}{2}\sigma_{i2(011)}^{(\alpha,1,\gamma)} + \left(\frac{h_1}{2}\right)^3 \sigma_{i2(031)}^{(\alpha,1,\gamma)} = -\frac{h_2}{2}\sigma_{i2(011)}^{(\alpha,2,\gamma)} - \left(\frac{h_2}{2}\right)^3 \sigma_{i2(031)}^{(\alpha,2,\gamma)} \tag{2.44}$$

$$\sigma_{i2(101)}^{(\alpha,1,\gamma)} + \left(\frac{h_1}{2}\right)^2 \sigma_{i2(121)}^{(\alpha,1,\gamma)} = \sigma_{i2(101)}^{(\alpha,2,\gamma)} + \left(\frac{h_2}{2}\right)^2 \sigma_{i2(121)}^{(\alpha,2,\gamma)} \tag{2.45}$$

$$\sigma_{i2(200)}^{(\alpha,1,\gamma)} + \left(\frac{h_1}{2}\right)^2 \sigma_{i2(220)}^{(\alpha,1,\gamma)} = \sigma_{i2(200)}^{(\alpha,2,\gamma)} + \left(\frac{h_2}{2}\right)^2 \sigma_{i2(220)}^{(\alpha,2,\gamma)} \tag{2.46}$$

$$\sigma_{i2(002)}^{(\alpha,1,\gamma)} + \left(\frac{h_1}{2}\right)^2 \sigma_{i2(022)}^{(\alpha,1,\gamma)} = \sigma_{i2(002)}^{(\alpha,2,\gamma)} + \left(\frac{h_2}{2}\right)^2 \sigma_{i2(022)}^{(\alpha,2,\gamma)} \tag{2.47}$$

Finally, for the interfaces with the normal in the x_3 direction have the following traction continuity equations

$$\sigma_{i3(000)}^{(\alpha,\beta,1)} + \left(\frac{l_1}{2}\right)^2 \sigma_{i3(002)}^{(\alpha,\beta,1)} + \left(\frac{l_1}{2}\right)^4 \sigma_{i3(004)}^{(\alpha,\beta,1)} = \sigma_{i3(000)}^{(\alpha,\beta,2)} + \left(\frac{l_2}{2}\right)^2 \sigma_{i3(002)}^{(\alpha,\beta,2)} + \left(\frac{l_2}{4}\right)^4 \sigma_{i3(004)}^{(\alpha,\beta,2)} \tag{2.48}$$

$$\frac{l_1}{2}\sigma_{i3(101)}^{(\alpha,\beta,1)} + \left(\frac{l_1}{2}\right)^3 \sigma_{i3(103)}^{(\alpha,\beta,1)} = -\frac{l_2}{2}\sigma_{i3(101)}^{(\alpha,\beta,2)} - \left(\frac{l_2}{2}\right)^3 \sigma_{i3(103)}^{(\alpha,\beta,2)} \tag{2.49}$$

$$\frac{l_1}{2}\sigma_{i3(011)}^{(\alpha,\beta,1)} + \left(\frac{l_1}{2}\right)^3 \sigma_{i3(013)}^{(\alpha,\beta,1)} = -\frac{l_2}{2}\sigma_{i3(011)}^{(\alpha,\beta,2)} - \left(\frac{l_2}{2}\right)^3 \sigma_{i3(013)}^{(\alpha,\beta,2)} \tag{2.50}$$

$$\sigma_{i3(110)}^{(\alpha,\beta,1)} + \left(\frac{l_1}{2}\right)^2 \sigma_{i3(112)}^{(\alpha,\beta,1)} = \sigma_{i3(110)}^{(\alpha,\beta,2)} \left(\frac{l_2}{2}\right)^2 \sigma_{i3(112)}^{(\alpha,\beta,2)} \tag{2.51}$$

$$\sigma_{i3(200)}^{(\alpha,\beta,1)} + \left(\frac{l_1}{2}\right)^2 \sigma_{i3(202)}^{(\alpha,\beta,1)} = \sigma_{i3(200)}^{(\alpha,\beta,2)} + \left(\frac{l_2}{2}\right)^2 \sigma_{i3(202)}^{(\alpha,\beta,2)} \tag{2.52}$$

$$\sigma_{i3(020)}^{(\alpha,\beta,1)} + \left(\frac{l_1}{2}\right)^2 \sigma_{i3(022)}^{(\alpha,\beta,1)} = \sigma_{i3(020)}^{(\alpha,\beta,2)} + \left(\frac{l_2}{2}\right)^2 \sigma_{i3(022)}^{(\alpha,\beta,2)} \tag{2.53}$$

The number of traction continuity equations of each different order is the same as for the displacement continuity equations. Hence there are a total of 216 governing traction continuity equations for the unit cell. As was the case for the displacement continuity equations, the above traction continuity equations satisfy the continuity constraints both within a unit cell as well as between unit cells, i.e. these equations identically satisfy all traction continuity constraints associated with the problem.

To this point in the formulation there are 312 equilibrium equations, and 216 displacement continuity constraints, and 216 traction continuity relations in the governing equation set or a total of 744 governing equations. There are 816 total unknown $V^{(\alpha,\beta,\gamma)}_{i(m,n,r)}$. Thus, an additional 72 governing equations are required to obtain a deterministic system of governing equations. The remaining governing equations are obtained from the following constraints

$$V^{(\alpha,\beta,\gamma)}_{i(221)} = 0 \tag{2.54}$$

$$V^{(\alpha,\beta,\gamma)}_{i(212)} = 0 \tag{2.55}$$

$$V^{(\alpha,\beta,\gamma)}_{i(122)} = 0 \tag{2.56}$$

These additional constraint equations are based on the fact that these terms do not appear explicitly in the above set of governing equations. This constraint can be physcially interpreted as meaning that these terms can not be supported within the context of the proposed orders of the fields. It is noted that in a higher order analysis these terms would be retained.

2.3. Implementation of the governing equations

The final system of governing equations, Eq. (2.5)–(2.56), provides the necessary system of 816 governing equations for determining the 816 unknown $V^{(\alpha,\beta,\gamma)}_{i(m,n,r)}$. These governing equations are algebraic in nature and thus can be directly assembled into matrix form by simply considering each governing equation to represent one line in the matrix equation. In particular, the displacement continuity equations, Eq. (2.18)–(2.35) are utilized as given. Once a given set of constitutive relations have been specified the stresses can be expressed directly in terms of the fundamental kinematic unknowns and, if appropriate, the eigenstrain effects using the process discussed in Section 2.1. Subsequent substitution of these results into the equilibrium equations, Eq. (2.5)–(2.17) and the traction continuity equations, Eq. (2.36)–(2.53) allows these governing equations to be expressed directly in terms of the unknowns. Under the assumption of linear elastic behavior the final system of governing equations has a form identical to that of the 2D theory, namely,

$$\underline{\underline{K}}\,\underline{V} = \underline{\underline{F}}\,\underline{\bar{\epsilon}} \tag{2.57}$$

In this equation the matrix $\underline{\underline{K}}$ is a coefficient matrix that is a function of the material and geometric properties of the subcells, the vector of unknowns for the unit cell is given by $\underline{V}$, the matrix $\underline{\underline{F}}$ is associated with the forcing terms and is a known function of the material and geometric properties of the subcells, and the vector $\underline{\bar{\epsilon}}$ represents the applied bulk loading. If the constituents are assumed to exhibit history-dependent responses then additional terms would appear in the above matrix equation. This extension to history-dependent effects will be addressed in future work.

2.4. Specialization of governing equations for orthotropic phases

Similarly to the 2D theory, the above results can be separated into four independent (smaller) groups of unknowns and associated governing equations in the case where the constituent materials are Hookean and exhibit at least orthotropic symmetry. The separation of the unknowns into these groups results in

enhanced computational efficiency. In the following discussion, the subscripts on the equation numbers indicates the appropriate value of the free index.

The first grouping is driven by the bulk shear strain $\overline{\epsilon}_{12}$. The associated kinematic unknowns in a subcell are $V_{1(010)}$, $V_{1(210)}$, $V_{1(012)}$, $V_{1(030)}$, $V_{1(410)}$, $V_{1(014)}$, $V_{1(230)}$, $V_{1(032)}$, $V_{1(212)}$, $V_{1(050)}$, $V_{2(100)}$, $V_{2(120)}$, $V_{2(102)}$, $V_{2(300)}$, $V_{2(140)}$, $V_{2(104)}$, $V_{2(320)}$, $V_{2(302)}$, $V_{2(122)}$, $V_{2(005)}$, $V_{3(111)}$, $V_{3(311)}$, $V_{3(131)}$, and $V_{3(113)}$. The corresponding governing equations are Eq. $2.5_{i=2}$, $2.6_{i=1}$, $2.9_{i=1}$, $2.11_{i=1}$, $2.12_{i=2}$, $2.13_{i=3}$, $2.14_{i=2}$, $2.16_{i=1}$, $2.17_{i=2}$, $2.18_{i=2}$, $2.19_{i=1}$, $2.21_{i=3}$, $2.22_{i=2}$, $2.23_{i=2}$, $2.24_{i=1}$, $2.25_{i=2}$, $2.27_{i=3}$, $2.28_{i=1}$, $2.29_{i=1}$, $2.31_{i=2}$, $2.32_{i=1}$, $2.33_{i=3}$, $2.36_{i=2}$, $2.37_{i=1}$, $2.39_{i=3}$, $2.40_{i=2}$, $2.41_{i=2}$, $2.42_{i=1}$, $2.43_{i=2}$, $2.45_{i=3}$, $2.46_{i=1}$, $2.47_{i=1}$, $2.49_{i=2}$, $2.50_{i=1}$, $2.51_{i=3}$, $2.55_{i=2}$, $2.56_{i=1}$.

The second grouping is associated with $\overline{\epsilon}_{13}$ and has the following kinematic unknowns; $V_{1(001)}$, $V_{1(201)}$, $V_{1(021)}$, $V_{1(003)}$, $V_{1(401)}$, $V_{1(041)}$, $V_{1(203)}$, $V_{1(023)}$, $V_{1(221)}$, $V_{1(005)}$, $V_{3(100)}$, $V_{3(120)}$, $V_{3(102)}$, $V_{3(300)}$, $V_{3(140)}$, $V_{3(104)}$, $V_{3(320)}$, $V_{3(302)}$, $V_{3(122)}$, $V_{3(500)}$, $V_{2(111)}$, $V_{2(311)}$, $V_{2(131)}$, and $V_{2(113)}$. The governing equations for this group are; Eq. $2.5_{i=3}$, $2.7_{i=1}$, $2.8_{i=1}$, $2.10_{i=1}$, $2.12_{i=3}$, $2.13_{i=2}$, $2.14_{i=3}$, $2.15_{i=1}$, $2.17_{i=3}$, $2.18_{i=3}$, $2.20_{i=1}$, $2.21_{i=2}$, $2.22_{i=3}$, $2.23_{i=3}$, $2.25_{i=3}$, $2.26_{i=1}$, $2.27_{i=2}$, $2.30_{i=1}$, $2.31_{i=3}$, $2.33_{i=2}$, $2.34_{i=1}$, $2.35_{i=1}$, $2.36_{i=3}$, $2.38_{i=1}$, $2.39_{i=2}$, $2.40_{i=3}$, $2.41_{i=3}$, $2.43_{i=3}$, $2.44_{i=1}$, $2.45_{i=2}$, $2.48_{i=1}$, $2.49_{i=3}$, $2.51_{i=2}$, $2.52_{i=1}$, $2.53_{i=1}$, $2.54_{i=1}$, $2.56_{i=3}$.

The third grouping is associated with the remaining bulk shearing behavior, namely, $\overline{\epsilon}_{23}$. The related kinematic unknowns are $V_{2(001)}$, $V_{2(201)}$, $V_{2(021)}$, $V_{2(003)}$, $V_{2(401)}$, $V_{2(041)}$, $V_{2(203)}$, $V_{2(023)}$, $V_{2(221)}$, $V_{2(005)}$, $V_{3(010)}$, $V_{3(210)}$, $V_{3(012)}$, $V_{3(030)}$, $V_{3(410)}$, $V_{3(014)}$, $V_{3(230)}$, $V_{3(032)}$, $V_{3(212)}$, $V_{3(050)}$, $V_{1(111)}$, $V_{1(311)}$, $V_{1(131)}$, and $V_{1(113)}$. The appropriate governing equations for group 3 are Eq. $2.6_{i=3}$, $2.7_{i=2}$, $2.8_{i=2}$, $2.9_{i=3}$, $2.10_{i=2}$, $2.11_{i=3}$, $2.13_{i=1}$, $2.15_{i=2}$, $2.16_{i=3}$, $2.19_{i=3}$, $2.20_{i=2}$, $2.21_{i=1}$, $2.24_{i=3}$, $2.26_{i=2}$, $2.27_{i=1}$, $2.28_{i=3}$, $2.29_{i=3}$, $2.30_{i=2}$, $2.32_{i=3}$, $2.33_{i=1}$, $2.34_{i=2}$, $2.35_{i=2}$, $2.37_{i=3}$, $2.38_{i=2}$, $2.39_{i=1}$, $2.42_{i=3}$, $2.44_{i=2}$, $2.45_{i=1}$, $2.46_{i=3}$, $2.47_{i=3}$, $2.48_{i=2}$, $2.50_{i=3}$, $2.51_{i=1}$, $2.52_{i=2}$, $2.53_{i=2}$, $2.54_{i=2}$, $2.55_{i=3}$.

Each of the above groups exhibits coupling between the different types of local shear and normal effects as well as between different local shearing effects. The shearing responses represent both the average response for the group as well as higher order behavior. The normal effects, on the other hand, only exists as higher order phenomena. The governing equations for groups 1–3 can be cast in a common form given by

$$\underline{\underline{k}}^{(n)}\underline{V}^{(n)} = \underline{f}^{(n)}\overline{\epsilon}_{(s)} \tag{2.58}$$

where the superscript "(n)" denotes the group number and the subscript "(s)" on the bulk strains is used to denote one of the bulk shear strains. The interpretations of the individual terms in Eq. (2.58) exactly parallel those of the terms in Eq. (2.57). Solving these matrix equations for the unknowns provides analytic, closed form expressions for the concentration factors, namely,

$$\underline{V}^{(n)} = \underline{a}^{(n)}\overline{\epsilon}_s \tag{2.59}$$

where the concentration factors, $\underline{a}^{(n)}$, are given by

$$\underline{a}^{(n)} = \underline{\underline{k}}^{(n)^{-1}}\underline{f}^{(n)} \tag{2.60}$$

The final independent grouping, group 4, is driven by the bulk normal deformations $(\overline{\epsilon}_{11}, \overline{\epsilon}_{22}, \overline{\epsilon}_{33})$ and has the following kinematic unknowns $V_{1(100)}$, $V_{1(120)}$, $V_{1(102)}$, $V_{1(300)}$, $V_{1(140)}$, $V_{1(104)}$, $V_{1(320)}$, $V_{1(302)}$, $V_{1(122)}$, $V_{1(500)}$, $V_{2(010)}$, $V_{2(210)}$, $V_{2(012)}$, $V_{2(030)}$, $V_{2(410)}$, $V_{2(014)}$, $V_{2(230)}$, $V_{2(032)}$, $V_{2(212)}$, $V_{2(050)}$, $V_{3(001)}$, $V_{3(201)}$, $V_{3(021)}$, $V_{3(003)}$, $V_{3(401)}$, $V_{3(041)}$, $V_{3(203)}$, $V_{3(023)}$, $V_{3(221)}$, and $V_{3(005)}$. The governing equations for this group are Eq. $2.5_{i=1}$, $2.6_{i=2}$, $2.7_{i=3}$, $2.8_{i=3}$, $2.9_{i=2}$, $2.10_{i=3}$, $2.11_{i=2}$, $2.12_{i=1}$, $2.14_{i=1}$, $2.15_{i=3}$, $2.16_{i=2}$, $2.17_{i=1}$, $2.18_{i=1}$, $2.19_{i=2}$, $2.20_{i=3}$, $2.22_{i=1}$, $2.23_{i=1}$, $2.24_{i=2}$, $2.25_{i=1}$,$2.26_{i=3}$, $2.28_{i=2}$, $2.29_{i=2}$, $2.30_{i=3}$, $2.31_{i=1}$, $2.32_{i=2}$, $2.34_{i=3}$, $2.35_{i=3}$, $2.36_{i=1}$, $2.37_{i=2}$, $2.38_{i=3}$, $2.40_{i=1}$, $2.41_{i=1}$, $2.42_{i=2}$,

$2.43_{i=1}$, $2.44_{i=3}$, $2.46_{i=2}$, $2.47_{i=2}$, $2.48_{i=3}$, $2.49_{i=1}$, $2.50_{i=2}$, $2.52_{i=3}$, $2.53_{i=3}$, $2.54_{i=3}$, $2.55_{i=2}$ and $2.56_{i=1}$. The system of governing equations for group 4 can be written in the following matrix form

$$\underline{\underline{k}}^{(4)}\underline{V}^{(4)} = \underline{\underline{f}}^{(4)}\overline{\underline{\epsilon}}_{(n)} \tag{2.61}$$

The interpretations of the individual terms in the equation directly parallel those used in the other groups except that the vector $\overline{\underline{\epsilon}}_{(n)}$ consists of the three bulk normal strains $\overline{\epsilon}_{11}$, $\overline{\epsilon}_{22}$, and $\overline{\epsilon}_{33}$. Solving this system of equations gives

$$\underline{V}^{(4)} = \underline{\underline{a}}^{(4)}\overline{\underline{\epsilon}}_{(n)} \tag{2.62}$$

where the concentration factors $\underline{\underline{a}}^{(4)}$ are given by

$$\underline{\underline{a}}^{(4)} = \underline{\underline{k}}^{(4)^{-1}}\underline{\underline{f}}^{(4)} \tag{2.63}$$

Using Eqs. (2.59) and (2.62) in conjunction with the strain-displacement relations the fluctuating strains $\mu_{ij(p,q,s)}^{(\alpha,\beta,\gamma)}$ can be expressed in terms of the applied bulk strains

$$\mu_{ij(p,q,s)}^{(\alpha,\beta,\gamma)} = A_{ijkl(p,q,s)}^{(\alpha,\beta,\gamma)}\overline{\epsilon}_{kl} \tag{2.64}$$

where the $A_{ijkl(p,q,s)}^{(\alpha,\beta,\gamma)}$ represent the concentration tensor effects and are functions of the previously determined vectors $\underline{a}^{(i)}$ for $i = 1, 2, 3$ and the matrix $\underline{\underline{a}}^{(4)}$.

2.5. Effective constitutive properties of the composite

The effective properties of the composite system are determined exactly as was done in the 2D theory (Williams, 2004). The final expressions developed in that work for a composite composed of Hookean materials are simply repeated here and thus the effective composite properties are given by

$$C_{ijkl}^{\text{eff}} = \overline{C}_{ijkl} + \overline{C'_{ijmn}A_{mnkl}} \tag{2.65}$$

where the C'_{ijmn} are the fluctuating stiffness tensor components and the A_{mnkl} (see Eq. (2.64)) are the components of the concentration tensor in the different subcells. Assuming spatially constant properties within each subcell allows the above expression to be simplified to

$$C_{ijkl}^{\text{eff}} = \overline{C}_{ijkl} + \overline{C'_{ijmn}A_{mnkl(000)}} \tag{2.66}$$

or, alternatively, to

$$C_{ijkl}^{\text{eff}} = \overline{C}_{ijkl} + \sum_{\alpha,\beta,\gamma} c_{(\alpha,\beta,\gamma)}C'^{(\alpha,\beta,\gamma)}_{ijmn}A^{(\alpha,\beta,\gamma)}_{mnkl(000)} \tag{2.67}$$

where the $c_{(\alpha,\,\beta,\,\gamma)}$ are the subcell volume fractions, i.e. the relative volume of each subcell with respect to the total volume of the unit cell. The effective engineering properties are obtained from the effective stiffnesses, Eq. (2.65)–(2.67), using standard relations.

3. Third order theory

The specialization of the fifth order theory to a third order theory is carried out next. First, all fifth order terms in the displacement expansion as well as all fourth order terms in the strain and stress field expansions

are eliminated. The subcell fields still retain the forms given in Eqs. (2.2)–(2.4); however, the maximum cumulative order $(m+n+r)$ in Eq. (2.2) is reduced to three while the maximum cumulative orders $(p+q+s)$ in Eqs. (2.3) and (2.4) become two. Due to the above reductions each subcell retains only 39 kinematic unknowns resulting in a total of 312 unknowns for the unit cell.

Due to the elimination of the higher order effects the only remaining equilibrium equations are Eqs. (2.5)–(2.7). Furthermore, the elimination of the fourth order stress effects reduces these equilibrium equations to the following simplified forms

$$3\sigma^{(\alpha,\beta,\gamma)}_{i1(200)} + \sigma^{(\alpha,\beta,\gamma)}_{i2(110)} + \sigma^{(\alpha,\beta,\gamma)}_{i3(101)} = 0 \tag{3.1}$$

$$\sigma^{(\alpha,\beta,\gamma)}_{i1(110)} + 3\sigma^{(\alpha,\beta,\gamma)}_{i2(020)} + \sigma^{(\alpha,\beta,\gamma)}_{i3(011)} = 0 \tag{3.2}$$

$$\sigma^{(\alpha,\beta,\gamma)}_{i1(101)} + \sigma^{(\alpha,\beta,\gamma)}_{i2(011)} + 3\sigma^{(\alpha,\beta,\gamma)}_{i3(002)} = 0 \tag{3.3}$$

These equilibrium equations provide 9 governing equations per subcell or a total of 72 governing equations for the unit cell.

The interfacial continuity constraints in the third order theory are imposed through a cumulative order of one. This is consistent with the 2D theory. The appropriately specialized forms of Eqs. (2.18)–(2.23), the displacement continuity equations on the faces with the normal in the x_1 direction, are

$$\frac{d_1}{2}V^{(1,\beta,\gamma)}_{i(100)} + \left(\frac{d_1}{2}\right)^3 V^{(1,\beta,\gamma)}_{i(300)} = -\frac{d_2}{2}V^{(2,\beta,\gamma)}_{i(100)} - \left(\frac{d_2}{2}\right)^3 V^{(2,\beta,\gamma)}_{i(300)} \tag{3.4}$$

$$V^{(1,\beta,\gamma)}_{i(010)} + \left(\frac{d_1}{2}\right)^2 V^{(1,\beta,\gamma)}_{i(210)} = V^{(2,\beta,\gamma)}_{i(010)} + \left(\frac{d_2}{2}\right)^2 V^{(2,\beta,\gamma)}_{i(210)} \tag{3.5}$$

$$V^{(1,\beta,\gamma)}_{i(001)} + \left(\frac{d_1}{2}\right)^2 V^{(1,\beta,\gamma)}_{i(201)} = V^{(2,\beta,\gamma)}_{i(001)} + \left(\frac{d_2}{2}\right)^2 V^{(2,\beta,\gamma)}_{i(201)} \tag{3.6}$$

Eqs. (2.24)–(2.29) reduce to

$$\frac{h_1}{2}V^{(\alpha,1,\gamma)}_{i(010)} + \left(\frac{h_1}{2}\right)^3 V^{(\alpha,1,\gamma)}_{i(030)} = -\frac{h_2}{2}V^{(\alpha,2,\gamma)}_{i(010)} - \left(\frac{h_2}{2}\right)^3 V^{(\alpha,2,\gamma)}_{i(030)} \tag{3.7}$$

$$V^{(\alpha,1,\gamma)}_{i(100)} + \left(\frac{h_1}{2}\right)^2 V^{(\alpha,1,\gamma)}_{i(120)} = V^{(\alpha,2,\gamma)}_{i(100)} + \left(\frac{h_2}{2}\right)^2 V^{(\alpha,2,\gamma)}_{i(120)} \tag{3.8}$$

$$V^{(\alpha,1,\gamma)}_{i(001)} + \left(\frac{h_1}{2}\right)^2 V^{(\alpha,1,\gamma)}_{i(021)} = V^{(\alpha,2,\gamma)}_{i(001)} + \left(\frac{h_2}{2}\right)^2 V^{(\alpha,2,\gamma)}_{i(021)} \tag{3.9}$$

The last set of displacement continuity equations, Eq. (2.30)–(2.35) become

$$\frac{l_1}{2}V^{(\alpha,\beta,1)}_{i(001)} + \left(\frac{l_1}{2}\right)^3 V^{(\alpha,\beta,1)}_{i(003)} = -\frac{l_2}{2}V^{(\alpha,\beta,2)}_{i(001)} - \left(\frac{l_2}{2}\right)^3 V^{(\alpha,\beta,2)}_{i(003)} \tag{3.10}$$

$$V^{(\alpha,\beta,1)}_{i(100)} + \left(\frac{l_1}{2}\right)^2 V^{(\alpha,\beta,1)}_{i(102)} = V^{(\alpha,\beta,2)}_{i(100)} + \left(\frac{l_2}{2}\right)^2 V^{(\alpha,\beta,2)}_{i(102)} \tag{3.11}$$

$$V^{(\alpha,\beta,1)}_{i(010)} + \left(\frac{l_1}{2}\right)^2 V^{(\alpha,\beta,1)}_{i(012)} = V^{(\alpha,\beta,2)}_{i(010)} + \left(\frac{l_2}{2}\right)^2 V^{(\alpha,\beta,2)}_{i(012)} \tag{3.12}$$

The above displacement continuity equations represent a system of 108 governing equations. The corresponding traction continuity conditions, Eq. (2.36)–(2.53), reduce to the following 108 governing equations

$$\sigma^{(1,\beta,\gamma)}_{i1(000)} + \left(\frac{d_1}{2}\right)^2 \sigma^{(1,\beta,\gamma)}_{i1(200)} = \sigma^{(2,\beta,\gamma)}_{i1(000)} + \left(\frac{d_2}{2}\right)^2 \sigma^{(2,\beta,\gamma)}_{i1(200)} \tag{3.13}$$

$$\frac{d_1}{2}\sigma^{(1,\beta,\gamma)}_{i1(110)} = -\frac{d_2}{2}\sigma^{(2,\beta,\gamma)}_{i1(110)} \tag{3.14}$$

$$\frac{d_1}{2}\sigma^{(1,\beta,\gamma)}_{i1(101)} = -\frac{d_2}{2}\sigma^{(2,\beta,\gamma)}_{i1(101)} \tag{3.15}$$

$$\sigma^{(\alpha,1,\gamma)}_{i2(000)} + \left(\frac{h_1}{2}\right)^2 \sigma^{(\alpha,1,\gamma)}_{i2(020)} = \sigma^{(\alpha,2,\gamma)}_{i2(000)} + \left(\frac{h_2}{2}\right)^2 \sigma^{(\alpha,2,\gamma)}_{i2(020)} \tag{3.16}$$

$$\frac{h_1}{2}\sigma^{(\alpha,1,\gamma)}_{i2(110)} = -\frac{h_2}{2}\sigma^{(\alpha,2,\gamma)}_{i2(110)} \tag{3.17}$$

$$\frac{h_1}{2}\sigma^{(\alpha,1,\gamma)}_{i2(011)} = -\frac{h_2}{2}\sigma^{(\alpha,2,\gamma)}_{i2(011)} \tag{3.18}$$

$$\sigma^{(\alpha,\beta,1)}_{i3(000)} + \left(\frac{l_1}{2}\right)^2 \sigma^{(\alpha,\beta,1)}_{i3(002)} = \sigma^{(\alpha,\beta,2)}_{i3(000)} + \left(\frac{l_2}{2}\right)^2 \sigma^{(\alpha,\beta,2)}_{i3(002)} \tag{3.19}$$

$$\frac{l_1}{2}\sigma^{(\alpha,\beta,1)}_{i3(101)} = -\frac{l_2}{2}\sigma^{(\alpha,\beta,2)}_{i3(101)} \tag{3.20}$$

$$\frac{l_1}{2}\sigma^{(\alpha,\beta,1)}_{i3(011)} = -\frac{l_2}{2}\sigma^{(\alpha,\beta,2)}_{i3(011)} \tag{3.21}$$

Consideration of Eqs. (3.14), (3.15), (3.17), (3.18), (3.20) and (3.21) shows that not all of the shearing forms of these equations are independent. In particular, one of Eqs. $(3.14)_{i=2}$ and $(3.17)_{i=1}$ for each index γ must be replaced by

$$\sum_{\alpha,\beta} d_\alpha^3 h_\beta^3 \left(V^{(\alpha,\beta,\gamma)}_{1(120)} - V^{(\alpha,\beta,\gamma)}_{2(210)}\right) = 0 \tag{3.22}$$

while one of Eqs. $(3.15)_{i=3}$ and $(3.20)_{i=1}$ for each index β is eliminated in favor of

$$\sum_{\alpha,\gamma} d_\alpha^3 l_\gamma^3 \left(V^{(\alpha,\beta,\gamma)}_{1(102)} - V^{(\alpha,\beta,\gamma)}_{3(201)}\right) = 0 \tag{3.23}$$

and, finally,

$$\sum_{\beta,\gamma} h_\beta^3 l_\gamma^3 \left(V^{(\alpha,\beta,\gamma)}_{2(012)} - V^{(\alpha,\beta,\gamma)}_{3(021)}\right) = 0 \tag{3.24}$$

replaces one of Eqs. $(3.18)_{i=3}$ and $(3.21)_{i=2}$ for each value of the index α. These spin constraints are based on the fact that an homogeneous material subjected to a deformation field of the form given by

Eq. (2.1) has zero spin. It is noted that imposing similar constraints on the average spins can be used to directly determine the individual kinematic unknowns in the original MOC theory.

To this point in the formulation there are 288 governing equations for 312 unknowns. Thus, an additional 24 governing equations are required to obtain a consistent system of governing equations and unknowns. As was the case for the fifth order theory, to obtain a consistent set of governing equations any terms that do not explicitly appear in the displacement continuity conditions, Eqs. (2.4)–(2.12), must be set to zero. Thus, this requirement imposes the following governing equation

$$V^{(\alpha,\beta,\gamma)}_{i(111)} = 0 \tag{3.25}$$

which represent the last required 24 governing equations.

Eqs. (3.1)–(3.25), represent 312 governing equations for the 312 unknown kinematic terms $V^{(\alpha,\beta,\gamma)}_{i(m,n,r)}$.

If Hookean behavior and, at least, orthotropic symmetry is assumed then the governing equations and the associated unknowns can be separated into four independent groups as was done in the 2D theory and the fifth order 3D theory.

The remaining unknowns for group 1 are $V_{1(010)}$, $V_{1(210)}$, $V_{1(012)}$, $V_{1(030)}$, $V_{2(100)}$, $V_{2(120)}$, $V_{2(102)}$, $V_{2(300)}$, and $V_{3(111)}$. The group governing equations become Eq. $3.1_{i=2}$, $3.2_{i=1}$, $3.4_{i=2}$, $3.5_{i=1}$, $3.1_{i=2}$, $3.7_{i=1}$, $3.8_{i=2}$, $3.1_{i=2}$, $3.11_{i=2}$, $3.12_{i=1}$, $3.13_{i=2}$, $3.14_{i=1}$, $3.16_{i=1}$, $3.17_{i=2}$, $3.1_{i=2}$, $3.20_{i=2}$ and $3.21_{i=1}$. The unknowns in group 2 are: $V_{1(001)}$, $V_{1(201)}$, $V_{1(021)}$, $V_{1(003)}$, $V_{3(100)}$, $V_{3(120)}$, $V_{3(102)}$, $V_{3(300)}$, and $V_{2(111)}$. The corresponding governing equations are Eq. $3.1_{i=3}$, $3.3_{i=1}$, $3.4_{i=3}$, $3.6_{i=1}$, $3.8_{i=3}$, $3.9_{i=1}$, $3.10_{i=1}$, $3.11_{i=3}$, $3.13_{i=3}$, $3.15_{i=1}$, $3.17_{i=3}$, $3.18_{i=1}$, $3.19_{i=1}$ and $3.20_{i=3}$. The unknowns in group 3 are $V_{2(001)}$, $V_{2(201)}$, $V_{2(021)}$, $V_{2(003)}$, $V_{3(010)}$, $V_{3(210)}$, $V_{3(012)}$, $V_{3(030)}$, and $V_{1(111)}$. The appropriate governing equations for group 3 are Eq. $3.2_{i=3}$, $3.3_{i=2}$, $3.5_{i=3}$, $3.6_{i=2}$, $3.1_{i=2}$, $3.7_{i=3}$, $3.9_{i=2}$, $3.10_{i=2}$, $3.12_{i=3}$, $3.14_{i=3}$, $3.15_{i=2}$, $3.16_{i=3}$, $3.18_{i=2}$, $3.19_{i=2}$ and $3.21_{i=3}$. Group 4 has the unknowns $V_{1(100)}$, $V_{1(120)}$, $V_{1(102)}$, $V_{1(300)}$, $V_{2(010)}$, $V_{2(210)}$, $V_{2(012)}$, $V_{2(030)}$, $V_{3(001)}$, $V_{3(201)}$, $V_{3(021)}$, and $V_{3(003)}$. The governing equations for group 4 are Eq. $3.1_{i=1}$, $3.2_{i=2}$, $3.3_{i=3}$, $3.4_{i=1}$, $3.5_{i=2}$, $3.6_{i=3}$, $3.7_{i=2}$, $3.8_{i=1}$, $3.9_{i=3}$, $3.10_{i=3}$, $3.11_{i=1}$, $3.12_{i=2}$, $3.13_{i=1}$, $3.14_{i=2}$, $3.15_{i=3}$, $3.16_{i=2}$, $3.17_{i=1}$, $3.18_{i=3}$, $3.19_{i=3}$, $3.20_{i=1}$ and $3.21_{i=2}$ where one of Eq. $(2.14)_{i=2}$ or Eq. $2.17_{i=1}$ is replaced by Eq. (3.22) and one of Eq. $(2.15)_{i=3}$ or Eq. $(2.20)_{i=1}$ is replaced by Eq. (3.23) and one of Eq. $(3.18)_{i=3}$ or Eq. $(3.21)_{i=2}$ is replaced by Eq. (3.24). These smaller systems of governing equations have the same forms as Eq. (2.58) or (2.61) and are obtained via a straight forward simplification of the previously specified groupings. The solutions for these reduced groups have the forms given by Eqs. (2.59), (2.60), (2.62) and (2.63). The appropriate form for the fluctuating strain field is identical to Eq. (2.64). Finally, the expressions given for the effective properties in the fifth order theory, Eqs. (2.65)–(2.67), are also appropriate for the third order theory.

4. Specialization of the higher order theories to the MOC theory

The original 3D MOC theory utilized a first order expansion for the subcell displacement field. Thus, a variant of this theory can be obtained by specializing the proposed higher order analyzes. In particular, all kinematic terms above the first order must be eliminated from the current approach. As a result of this elimination process all of the subcell equilibrium equations disappear. The continuity conditions across the interfaces are only applied through the zeroth order. The resulting system of governing equations and unknowns is consistent with Aboudi's original formulation. This reduction process implies that the 3D MOC theory can be considered to be a lowest order elasticity based analysis rather than a weak formulation.

5. Validation results

This section is intended to validate the proposed 3D theory. In particular, the predictions obtained from the model are compared to selected results in the open literature. In the following comparisons the current model will be referred as the ECM (elasticity-based cell model). The predictions obtained from the method of cells (MOC) are also given in some cases.

A necessary condition in the validation process of the 3D ECM is that it identically collapses down to the corresponding 2D ECM as well as collapsing down to the exact one dimensional solution (Aboudi, 1991). Numerical calculations show that the 3D theory does correctly reduce to both the 2D and 1D solutions such that the results in each case are the same (not shown).

The ability of the 3D theory to reproduce the 2D theory results means that all of the validation process applied to the 2D formulation also applies to the 3D analysis. In particular, the local fields predicted by the third and fifth order 3D ECM for a *W*/*Cu* composite are exactly the values quoted for the 2D ECM (Williams, 2004). To avoid repetition, only a single example of the comparison between the local fields predicted by the 3D ECM and the Green's function based solution of Walker et al. (1993) is presented to show the ECM's ability to accurately predict the local fields, Fig. 2. The fiber volume fraction used in this example is 0.5102. The heavy solid lines are the boundaries of the unit cell, the heavy dashed lines represent the boundaries of the subcells, and the light dashed lines represent the subregions within each subcell used in the G-F calculations. The first number in a subregion is the value obtained from the G-F analysis, the second is the prediction from the third order ECM, and the last value is the fifth order ECM prediction. All errors discussed below are referenced to the G-F solution. As can be seen both version of the ECM predict local fields that are in good agreement with the fields obtained from the Green's function analysis (Walker et al., 1993). A more detailed discussion of the comparison of the distributions in the local fields obtained from the two approaches at other volume fractions (ranging from approximately 2% to 75%) is given by Williams (2004). Note that the square inclusion problem represents a stringent test of a theory's ability

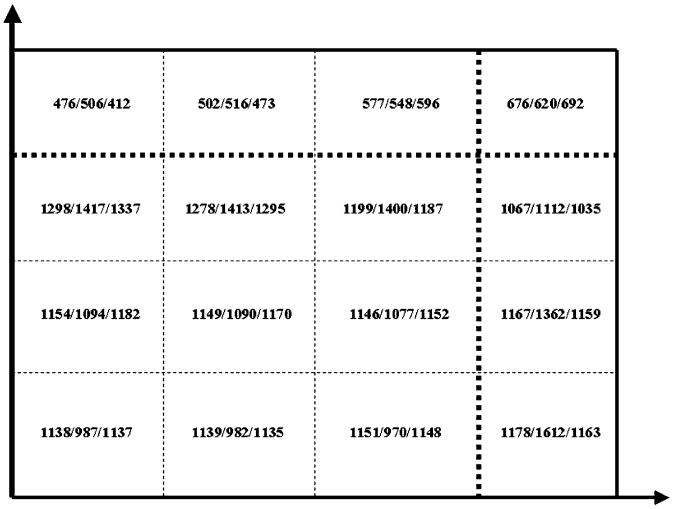

Fig. 2. The local stress field predictions from the Green's function analysis and both versions of the ECM for a *W*/*Cu* composite with a fiber volume of 0.5102. The heavy dashed lines represent the boundaries of the subcells in the ECM model. The fine dashed lines represent the boundaries of the computational cells used in the Green's function analysis. With regard to the ordering of the predictions, the first number in each triplet in each GF computational cell is the Green's function prediction, the second number is the third order ECM prediction, and the last number is the fifth order ECM prediction.

to correctly model the local and global behavior of a composite due to the presence of the strong gradients in the local fields induced by the presence of corners.

Now the 3D ECM's ability to predict the effective properties of particulate composites is considered. The model's predictions are compared to the predictions of Banks-Sills et al. (1997). The results of Banks-Sills et al. (1997) are derived by using the asymptotic homogenization theory (Bensoussan et al., 1978) in conjunction with finite elements (FE). In the following discussion this approach is referred to as the HFE method. Banks-Sills et al. validated the HFE approach through comparisons with both conventional finite elements analyzes as well as analytical homogenization models. The HFE approach can be considered to be a FE analysis based on the use of periodic fields and boundary conditions. All of the HFE results where generated based on converged meshes. It is noted that for the following examples that consider the bulk effective properties the ECM results are independent of the loading state. This is unlike FE based analyzes that require the implementation of six independent loading states in order to determine the effective properties. Finally, it is noted that the results are generated using volume fraction ranges that are consistent with typical inclusion volume fractions for particulate composites. The ability of the modeling approach to deal with higher volume fraction cases has been illustrated in Williams (2004) (see preceeding paragraph).

The first comparison between the ECM and the HFE method is for the effective Young's modulus as a function of inclusion volume fraction for a *Gl*/*Ep* system (the constituent properties are given in Table 1), Fig. 3. For this example the microstructure is composed of spheres embedded in a triply periodic cubic array. The third order ECM provides predictions that are in good agreement with the hexagonal array

Table 1
Properties for glass and epoxy constituents (Banks-Sills et al., 1997)

Material	E (GPa)	ν	G (GPa)
Glass (Gl)	76.00	0.23	30.89
Epoxy (Ep)	3.01	0.394	1.08

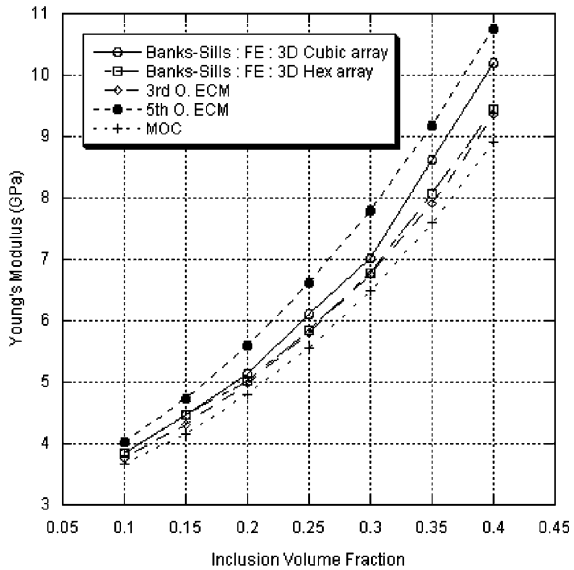

Fig. 3. Predictions for the effective Young's modulus as a function of inclusion volume fraction for a *Gl*/*Ep* composite with spherical inclusions.

Table 2
Properties for Al_2O_3 and aluminum constituents (Banks-Sills et al., 1997)

Material	E (GPa)	ν	G (GPa)
Aluminum oxide (Al_2O_3)	350.00	0.30	134.61
Aluminum (Al)	70.00	0.30	26.92

calculations of the HFE method with the correlation improving as the volume fraction increases. The corresponding MOC results fall noticeably below the HFE predictions while the 5th order ECM predicts values of the effective modulus that are greater than both the square and hexagonal array HFE calculations. As the inclusion volume fraction increases the HFE predictions obtained using a square array begin to approach the 5th order ECM results. Based on the trends observed by Banks-Sills et al. (1997) that show cubic inclusions to produce a composite with a greater effective Young's modulus than does a spherical inclusion at the same volume fraction it can be concluded that the 5th order ECM corresponds to a model for a rectangular parallelepiped while the 3rd order ECM falls somewhere between modeling a rectangular parallelepiped inclusion and a spherical inclusion.

Next comparisons of the predictions obtained from the ECM and HFE method (as well as the MOC theory) for various moduli as a function of inclusion volume fraction for an Al_2O_3/Al composite with cubic inclusions in a square array are considered. The HFE analysis utilized 681 nodal points. The constituents material properties are given in Table 2. First, the results for the effective Young's modulus are examined, Fig. 4. The fifth order ECM and HFE results are nearly identical. The third order ECM values fall somewhat below these results (maximum error of 3.1% at a volume faction of 0.3) and the MOC results exhibit an error of 5%. Consideration of the effective Poisson's ratio, Fig. 5, shows that again the fifth order ECM provides predictions that are in excellent agreement with the HFE results (with an error of no more than 0.04%). Both the third order ECM and the MOC model exhibit greater degrees of error in their predictions (2.6% and 1.5%, respectively). It is interesting to note that the MOC model provides somewhat better predictions for this effective property than does the third order ECM. However, given the relatively small er-

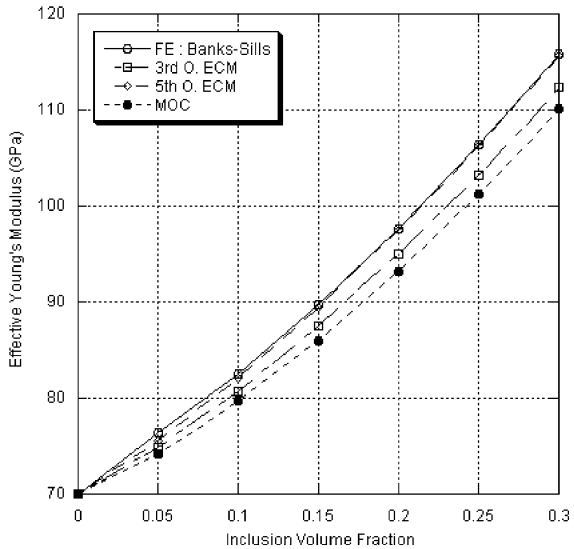

Fig. 4. Predictions for the effective Young's modulus as a function of inclusion volume fraction for an Al_2O_3/Al composite with cubic inclusions.

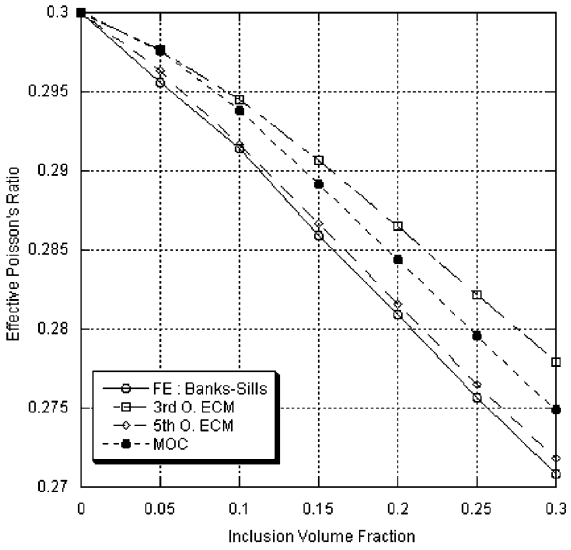

Fig. 5. Predictions for the effective Poisson's ratio as a function of inclusion volume fraction for an Al_2O_3/Al composite with cubic inclusions.

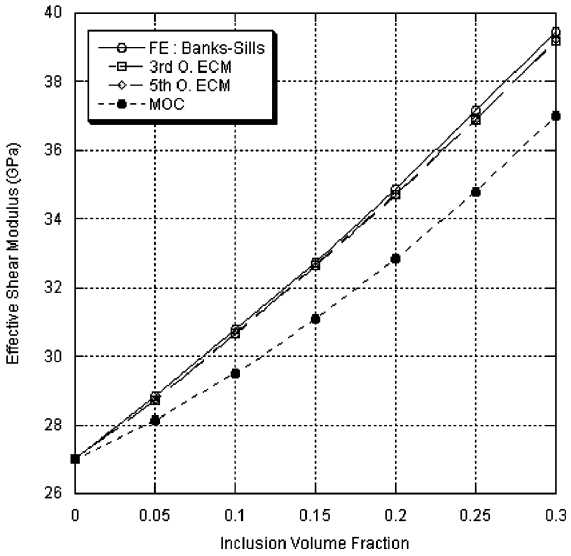

Fig. 6. Predictions for the effective shear modulus as a function of inclusion volume fraction for an Al_2O_3/Al composite with cubic inclusions.

rors in the predictions this trend is more an academic than a practical consideration. Finally, the predictions for the effective shear modulus are examined, Fig. 6. Both versions of the ECM provide predictions that are in excellent agreement with the HFE results with an error of no more than 0.6%. Alternatively, the MOC theory predicts moduli that exhibit errors of up to 6.2%.

The convergence of the average concentration factors for the above case at a inclusion volume fraction of 0.3 as a function of the order of the ECM solution used, i.e. first (MOC), third, or fifth order variant, is

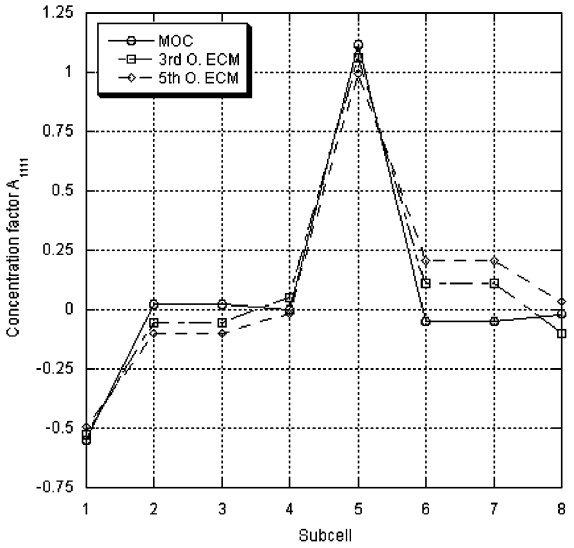

Fig. 7. The variation in the average concentration tensor $A_{1111(000)}$ as a function of subcell in the unit cell.

considered next. Because these results are based solely on the consideration of the concentration tensors they are independent of any particular loading state. Hence, these results indicate the convergence characteristics of the modeling approach as a function of the order of the expansions in the ECM. For this case there are essentially three different types of average concentration factors; one that relates the normal fluctuating strains to the same type of average strain, one that relates the normal fluctuating strains to the other types of average strains, and one that relates the fluctuating shear strains to the corresponding average shear strain. The following discussion will consider the first and third kind of concentration factors. In the rest of this paragraph and in the associated figures the following numbering scheme is used to denote the different subcells; subcell 111, 112, 121, 122, 211, 212, 221, and 222 are denoted by 1, 2, 3, 4, 5, 6, 7, and 8, respectively (see Fig. 1). The behavior of the concentration factor A_{1111} in the different subcells is considered first, Fig. 7. Generally speaking the variations in the concentration terms are due to the location of a given subcell within the microstructure and resultant interaction effects between the different subcells. Consideration of these results shows that for all but two of the subcells the convergence behavior is monotonic and progresses from the first order to the fifth order results. In the columns of subcells in the x_1 direction adjacent to the column containing the inclusion (in the x_2 and x_3 directions) these progressions involve a sign change in the concentration factor such that the MOC results are of one sign and the third and fifth order ECM predictions take the other sign. In these cases the differences between the MOC and the third order ECM results are almost twice that of the differences between the third and fifth order ECM solutions. For the column in the x_1 direction that contains the inclusion, the evolution of the results is the same but with smaller changes in magnitude and with less variation in the differences. In the case of the column of subcells (in the x_1 direction) containing the 122 and 222 (denoted by 4 and 8 respectively in the figure) subcells the evolution of the solutions is not monotonic. This indicates that the solution may not be converged in these subcells and to achieve convergence higher order ECM solutions may be required. However, given the fact that the fifth order ECM solutions in these subcells are substantially smaller than the fifth order ECM solutions for the next smallest concentration factor (in subcells 2 or 3) this lack of convergence may be of academic interest only and is not expected to practically impact the predicted bulk behavior. Further support that the fifth order ECM provides a nearly converged solution is given by the fidelity of the model's predictions for the local fields, (see Fig. 2 and Williams (2004)). Note that the above discussion for

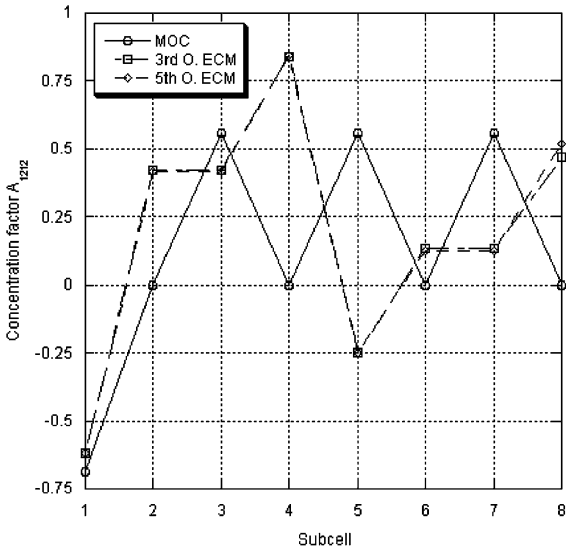

Fig. 8. The variation in the average concentration tensor $A_{1212(000)}$ as a function of subcell in the unit cell.

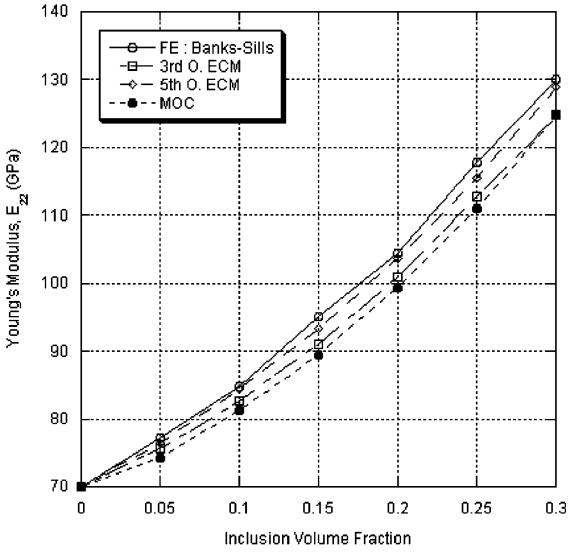

Fig. 9. Predictions for the effective Young's modulus E_{22} as a function of inclusion volume fraction for an Al_2O_3/Al composite with rectangular parallelepiped inclusions.

A_{1111} also applies to the concentration factors A_{2222} and A_{3333} when appropriate changes in direction are applied. Next, the convergence characteristics for the shear concentration terms are examined, Fig. 8. Note that all of the average shear concentration factors are the same for the current microstructure. Consideration shows that the third and fifth order ECM solutions are identical or nearly identical for all subcells. Thus, the fifth order solution can be considered to represent a converged solution for the shearing response. The predictions for these concentration factors obtained from the first order (MOC) solution, however, exhibit substantial differences from the higher order ECM solutions. The differences are due to the first order

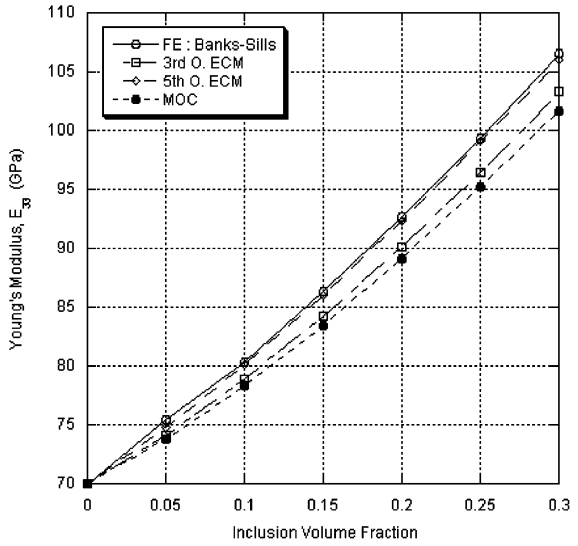

Fig. 10. Predictions for the effective Young's modulus E_{33} as a function of inclusion volume fraction for an Al_2O_3/Al composite with rectangular parallelepiped inclusions.

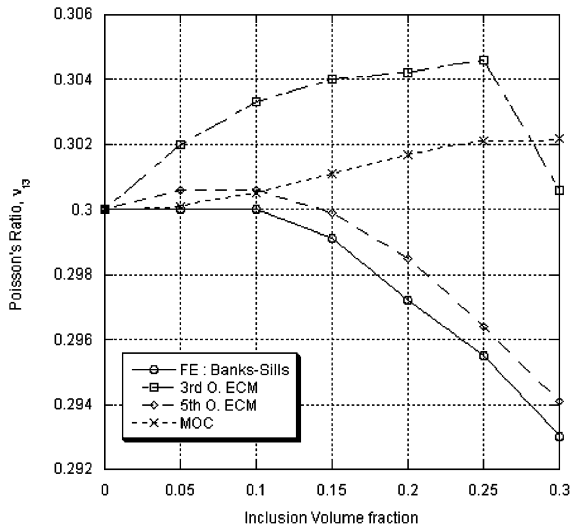

Fig. 11. Predictions for the effective Poisson's ratio v_{13} as a function of inclusion volume fraction for an Al_2O_3/Al composite with rectangular parallelepiped inclusions.

solution's inability to predict nonzero concentration factors which in turn is due to a lack of coupling phenomena in the local fields. This result emphasizes the importance of incorporating coupling effects in the ECM.

The final set of comparisons based on the Banks-Sills et al. (1997) results are for a unit cell with a rectangular parallelepiped inclusion where $d_1 = h_1 = 2a$ and $l_1 = a$ and a is calculated for a given inclusion volume fraction. The inclusions and the matrix are the previously considered Al_2O_3 and Al materials, Table 2. The HFE analysis is based on the use of 1295 nodal points in this case. The predictions for the Young's

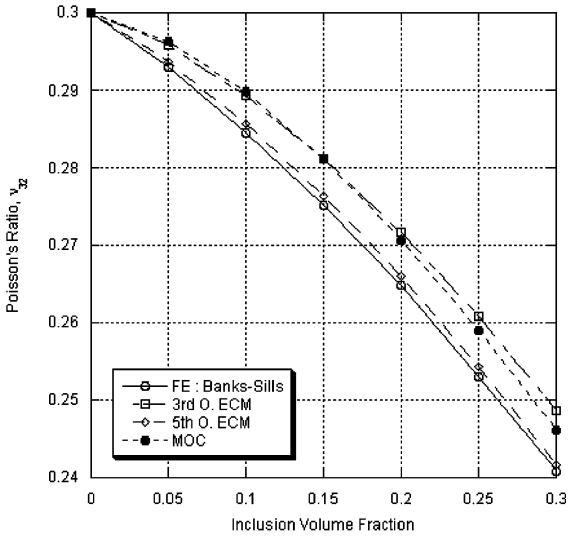

Fig. 12. Predictions for the effective Poisson's ratio ν_{32} as a function of inclusion volume fraction for an Al_2O_3/Al composite with rectangular parallelepiped inclusions.

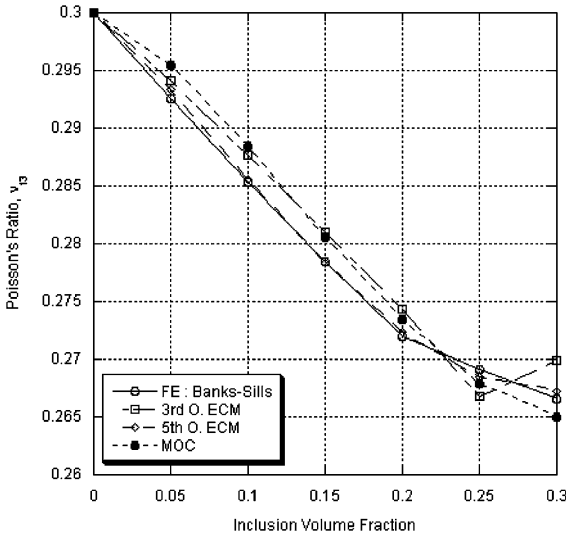

Fig. 13. Predictions for the effective Poisson's ratio ν_{12} as a function of inclusion volume fraction for an Al_2O_3/Al composite with rectangular parallelepiped inclusions.

modulus E_{22} and E_{33} are given in Figs. 9 and 10, respectively. The fifth order ECM provides predictions in both cases that are in very good agreement with the HFE data with errors of no more than 0.7%. The third order ECM gives the next most accurate predictions for both moduli with a maximum error of about 4%. The MOC theory gives the least accurate values although as the inclusion volume fraction increases the MOC values approach and ultimately coincide with the third order ECM results. Next the predictions for the major Poisson's ratio, ν_{13} is considered, Fig. 11. Again the fifth order ECM provides values that are in excellent agreement with the HFE results with errors of less than 0.4%. The third order ECM gives

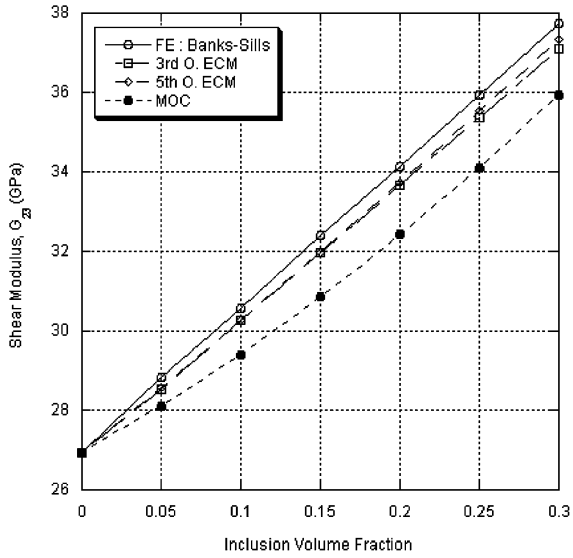

Fig. 14. Predictions for the effective shear modulus G_{23} as a function of inclusion volume fraction for an Al_2O_3/Al composite with rectangular parallelepiped inclusions.

the least accurate results at lower inclusion volume fractions but as the volume fraction increases this model provides more accurate predictions than the MOC model. The errors in this model's predictions are less than 1.8%. Examination of the predictions for the minor Poisson's ratio, v_{32}, Fig. 12, shows that the trends observed with respect to the major Poisson's ratio continue to hold, i.e. the fifth order ECM gives the most accurate prediction (with errors of less than 0.35%) while the third order ECM's values are the least accurate and exhibit maximum errors of approximately 3%. The results for the major Poisson's ratio v_{12} are given in Fig. 13. The predictions obtained using the fifth order ECM are in excellent agreement with the HFE results and exhibit errors that are relatively insignificant. Unlike the situations with the previous Poisson's ratios the third order ECM results are more accurate than the MOC calculations at lower volume fractions but exhibit greater degrees of error than the MOC data at higher inclusion fractions. It is noted that the errors observed in the MOC and third order ECM results are less than 1.5%. Finally, the estimates for the shear modulus G_{23} are evaluated, Fig. 14. The third and fifth order ECM calculations are essentially identical at lower inclusion fractions but as the volume fraction increases the fifth order theory is capable of providing slightly more accurate estimates than the third order theory. Both versions of the ECM are significantly more accurate than the MOC model, errors of 1% for the fifth order ECM as compared to errors of 5% for the MOC model at a volume fraction of 0.30. The trends in the predictions for the shear modulus G_{12} are similar to those observed in the behavior of G_{23}.

As a final comparison, the predictions for the local stresses obtained from the fifth order ECM and a finite element (FE) simulation (ABAQUS) are compared. The microstructure is composed of a cubic inclusion of silicon carbide embedded in an aluminum matrix. The inclusion volume fraction is 34.3%. It is noted

Table 3
Properties for SiC and aluminum constituents

Material	E (GPa)	v	G (GPa)
Silicon Carbide (SiC)	414.00	0.30	159.23
Aluminum (Al)	72.40	0.33	27.22

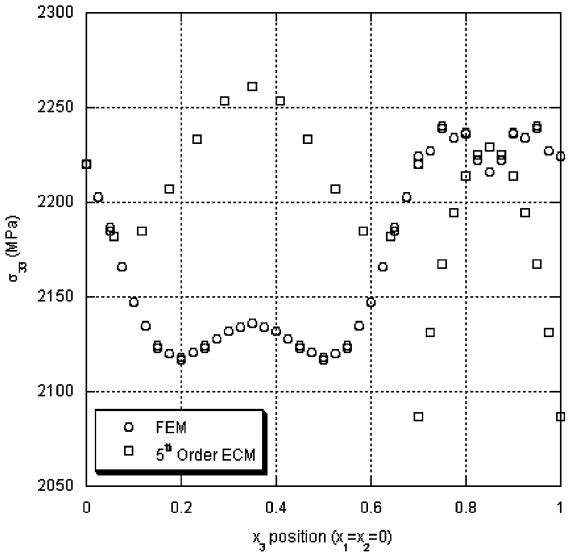

Fig. 15. Predictions for the local stress as a function of position along the centerline parallel to the applied loading.

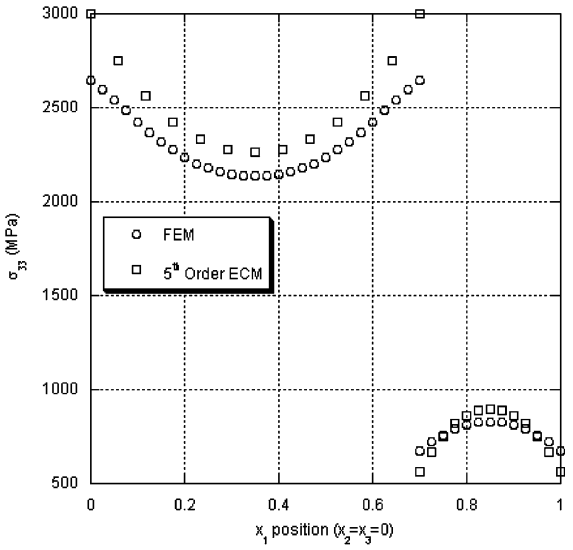

Fig. 16. Predictions for the local stress as a function of position along the centerline perpendicular to the applied loading.

that the current case represents a situation with a relatively high loading of inclusions and, thus, relatively strong interactions between inclusions. The properties of the individual phases are given in Table 3. The composite is subjected to a uniaxial strain of 1.0%. This loading state represents the complimentary loading state to the uniaxial stress states considered in the previous examples. The finite element simulation is based on a $20 \times 20 \times 20$ mesh of 20 noded quadratic elements (107163 degrees of freedom). First, consider the distributions of the local stress on the centerline along the direction of loading, Fig. 15. The overall spatial distribution trends in the FE and ECM results in the inclusion are the same. In particular, in the region

nearest to the interfaces the predicted stress states decrease. At greater distances from the interfaces this trend is reverse and both analyses predict an increasing state of stress. The ECM values near the boundaries of the inclusion are in excellent agreement with the FE values in this region. Towards the interior of the inclusion the ECM results are higher than those obtained from the FE analysis. The greatest difference in the predictions in the inclusion between the two analyses is less than 6%. In the matrix the ECM predictions do not show as close an agreement with the FE results. In particular, the rapid fluctuations in the FE results are not accurately captured by the ECM. However, the greatest differences in the predictions are less than 7%. It is expected that a higher order analysis would be required to adequately capture these features in the microlevel response. Now consider the distribution of the local stress along the centerline perpendicular to the applied loading state, Fig. 16. The trends in the predictions in both the matrix and the inclusions obtained from the two analyses are in good agreement. In particular, both analyses predict roughly parabolic distributions of the stress in the inclusion and the matrix with the stresses in the inclusion being substantially higher than in the matrix. In the inclusion the greatest differences between the two sets of predictions occur near the interfaces and are 12% or less. These differences decrease to around 6% at the middle of the inclusion. In matrix the greatest differences (less than 13%) also occur near the interfaces. It is noted that the matrix stresses in this region are those with the smallest magnitude for this distribution.

6. Summary and conclusion

The three-dimensional version of a new homogenization theory that employs a higher-order, elasticity based cell analysis has been presented. The formulation starts with a simplification of the microstructure for a 3D periodic array of inclusions. This simplified version of the material microstructure is consistent with that originally proposed by Aboudi (1991). Eigenfunction expansions truncated at a cumulative order of five are utilized to represent the displacement field in the different subcells of the discretized microstructure. Based on these displacement fields the theory directly satisfies the pointwise (strong) form of the governing equations of geometrically linear continuum mechanics up through an order consistent with the truncated expansions. The analysis is carried out independently of any constitutive assumptions for the individual constituents in the sense that the governing equations are valid for all constitutive theories. The proposed fifth order theory can be easily reduced to both third and first order theories. The first order version of this theory is consistent with the original method of cells (MOC) analysis proposed by Aboudi (1991). In fact, the current formulation shows that the original 3D MOC model can be reinterpreted as a lowest order elasticity solution rather than a weak formulation as originally suggested.

Comparisons with a wide variety of results from the open literature obtained using finite element based methodologies and Green's function analyzes have been carried out. These comparisons show that the proposed modeling approach is capable of providing accurate predictions for the local and global responses of one, two, and three-dimensional composites. This ability to provide accurate predictions shows that the proposed model provides a viable homogenization tool for the analysis of particulate composite materials as well as continuous fiber and bilaminated composites. Of the two variants proposed in the current work the fifth (cumulative) order version provides the most accurate predictions for both the local and global behavior. Additionally, it was shown that the incorporation of coupling effects in the local fields was necessary to improve the accuracy of the predictions as compared to the original 3D MOC theory predictions. Predictions for the convergence of the average local fields as a function of the order of the ECM theory have also been presented. It was shown that the first order theory may not adequately represent the local average fields. However, by increasing the order of the theory convergence in the predictions for the local fields is being achieved. Some of the results indicate that highly accurate representations of the local fields may require even higher order approximations than fifth order.

One of the most important contributions of the current work is that it represents the necessary theoretical foundations for the development of exact homogenization solutions of generalized, three-dimensional microstructures. While the proposed model has been shown to provide good estimates for the local response it can certainly be expected that higher order expansions and/or greater degrees of refinement in discretizing the material microstructure will lead to improved accuracy for predicting the local fields. The extension of the theory to both higher order approximations and arbitrary microstructural discretizations will be carried out in future work.

Appendix A

This appendix contains the expanded forms of the various field expansions and the definitions for the fluctuating strain effects (the $\mu_{ij(mn)}$). Note that in the following equations the superscript (α,β,γ) has been dropped since it is to be understood that the expressions apply to all subcells.

The expanded form of the displacement within a subcell for the fifth order theory is given by

$$\begin{aligned} u_i = {} & \bar{\epsilon}_{ij}x_j + P_{(100)}V_{i(100)} + P_{(010)}V_{i(010)} + P_{(001)}V_{i(001)} + P_{(003)}V_{i(003)} + P_{(012)}V_{i(012)} + P_{(021)}V_{i(021)} \\ & + P_{(030)}V_{i(030)} + P_{(102)}V_{i(102)} + P_{(111)}V_{i(111)} + P_{(120)}V_{i(120)} + P_{(201)}V_{i(201)} + P_{(210)}V_{i(210)} \\ & + P_{(300)}V_{i(300)} + P_{(005)}V_{i(005)} + P_{(014)}V_{i(014)} + P_{(023)}V_{i(023)} + P_{(032)}V_{i(032)} + P_{(041)}V_{i(041)} \\ & + P_{(050)}V_{i(050)} + P_{(104)}V_{i(104)} + P_{(113)}V_{i(113)} + P_{(122)}V_{i(122)} + P_{(131)}V_{i(131)} + P_{(140)}V_{i(140)} \\ & + P_{(203)}V_{i(203)} + P_{(212)}V_{i(212)} + P_{(221)}V_{i(221)} + P_{(230)}V_{i(230)} + P_{(302)}V_{i(302)} + P_{(311)}V_{i(311)} \\ & + P_{(320)}V_{i(320)} + P_{(401)}V_{i(401)} + P_{(410)}V_{i(410)} + P_{(500)}V_{i(500)} \end{aligned} \tag{A.1}$$

The corresponding strain field is

$$\begin{aligned} \epsilon_{ij} = {} & P_{(000)}(\bar{\epsilon}_{ij} + \mu_{ij(000)}) + P_{(002)}\mu_{ij(002)} + P_{(011)}\mu_{ij(011)} + P_{(020)}\mu_{ij(020)} + P_{(101)}\mu_{ij(101)} + P_{(110)}\mu_{ij(110)} \\ & + P_{(200)}\mu_{ij(200)} + P_{(004)}\mu_{ij(004)} + P_{(013)}\mu_{ij(013)} + P_{(022)}\mu_{ij(022)} + P_{(031)}\mu_{ij(031)} + P_{(040)}\mu_{ij(040)} \\ & + P_{(103)}\mu_{ij(103)} + P_{(112)}\mu_{ij(112)} + P_{(121)}\mu_{ij(121)} + P_{(130)}\mu_{ij(130)} + P_{(202)}\mu_{ij(202)} + P_{(211)}\mu_{ij(211)} \\ & + P_{(220)}\mu_{ij(220)} + P_{(301)}\mu_{ij(301)} + P_{(310)}\mu_{ij(310)} + P_{(400)}\mu_{ij(400)} \end{aligned} \tag{A.2}$$

and the associated subcell stress field is

$$\begin{aligned} \sigma_{ij} = {} & P_{(000)}\sigma_{ij(000)} + P_{(002)}\sigma_{ij(002)} + P_{(011)}\sigma_{ij(011)} + P_{(020)}\sigma_{ij(020)} + P_{(101)}\sigma_{ij(101)} + P_{(110)}\sigma_{ij(110)} \\ & + P_{(200)}\sigma_{ij(200)} + P_{(004)}\sigma_{ij(004)} + P_{(013)}\sigma_{ij(013)} + P_{(022)}\sigma_{ij(022)} + P_{(031)}\sigma_{ij(031)} + P_{(040)}\sigma_{ij(040)} \\ & + P_{(103)}\sigma_{ij(103)} + P_{(112)}\sigma_{ij(112)} + P_{(121)}\sigma_{ij(121)} + P_{(130)}\sigma_{ij(130)} + P_{(202)}\sigma_{ij(202)} + P_{(211)}\sigma_{ij(211)} \\ & + P_{(220)}\sigma_{ij(220)} + P_{(301)}\sigma_{ij(301)} + P_{(310)}\sigma_{ij(310)} + P_{(400)}\sigma_{ij(400)} \end{aligned} \tag{A.3}$$

The appropriate expressions for the fifth order fluctuating strains in the subcells are

$$\mu_{11(000)} = V_{1(100)} + \left(\frac{d_\alpha}{2}\right)^2 V_{1(300)} + \left(\frac{d_\alpha}{2}\right)^4 V_{1(500)}$$

$$\mu_{11(002)} = V_{1(102)} + \left(\frac{d_\alpha}{2}\right)^2 V_{1(302)}$$

$$\mu_{11(011)} = V_{1(111)} + \left(\frac{d_\alpha}{2}\right)^2 V_{1(311)}$$

$$\mu_{11(020)} = V_{1(120)} + \left(\frac{d_\alpha}{2}\right)^2 V_{1(320)}$$

$$\mu_{11(101)} = 3V_{1(201)} + 3\left(\frac{d_\alpha}{2}\right)^2 V_{1(401)}$$

$$\mu_{11(110)} = 3V_{1(210)} + 3\left(\frac{d_\alpha}{2}\right)^2 V_{1(410)}$$

$$\mu_{11(200)} = 5V_{1(300)} + 5\left(\frac{d_\alpha}{2}\right)^2 V_{1(500)}$$

$$\mu_{11(004)} = V_{1(104)}$$

$$\mu_{11(013)} = V_{1(113)}$$

$$\mu_{11(022)} = V_{1(122)}$$

$$\mu_{11(031)} = V_{1(131)}$$

$$\mu_{11(040)} = V_{1(140)}$$

$$\mu_{11(103)} = 3V_{1(203)}$$

$$\mu_{11(112)} = 3V_{1(212)}$$

$$\mu_{11(121)} = 3V_{1(221)}$$

$$\mu_{11(130)} = 3V_{1(230)}$$

$$\mu_{11(202)} = 5V_{1(302)}$$

$$\mu_{11(211)} = 5V_{1(311)}$$

$$\mu_{11(220)} = 5V_{1(320)}$$

$$\mu_{11(301)} = 7V_{1(401)}$$

$$\mu_{11(310)} = 7V_{1(410)}$$

$$\mu_{11(400)} = 9V_{1(500)}$$

$$\mu_{22(000)} = V_{2(010)} + \left(\frac{h_\beta}{2}\right)^2 V_{2(030)} + \left(\frac{h_\beta}{2}\right)^4 V_{2(050)}$$

$$\mu_{22(002)} = V_{2(012)} + \left(\frac{h_\beta}{2}\right)^2 V_{2(032)}$$

$$\mu_{22(011)} = 3V_{2(021)} + 3\left(\frac{h_\beta}{2}\right)^2 V_{2(041)}$$

$$\mu_{22(020)} = 5V_{2(030)} + 5\left(\frac{h_\beta}{2}\right)^2 V_{2(050)}$$

$$\mu_{22(101)} = V_{2(111)} + \left(\frac{h_\beta}{2}\right)^2 V_{2(131)}$$

$$\mu_{22(110)} = 3V_{2(120)} + 3\left(\frac{h_\beta}{2}\right)^2 V_{2(140)}$$

$$\mu_{22(200)} = V_{2(210)} + \left(\frac{h_\beta}{2}\right)^2 V_{2(230)}$$

$$\mu_{22(004)} = V_{2(014)}$$

$$\mu_{22(013)} = 3V_{2(023)}$$

$$\mu_{22(022)} = 5V_{2(032)}$$

$$\mu_{22(031)} = 7V_{2(041)}$$

$$\mu_{22(040)} = 9V_{2(050)}$$

$$\mu_{22(103)} = V_{2(113)}$$

$$\mu_{22(112)} = 3V_{2(122)}$$

$$\mu_{22(121)} = 5V_{2(131)}$$

$$\mu_{22(130)} = 7V_{2(140)}$$

$$\mu_{22(202)} = V_{2(212)}$$

$$\mu_{22(211)} = 3V_{2(221)}$$

$$\mu_{22(220)} = 5V_{2(230)}$$

$$\mu_{22(301)} = V_{2(311)}$$

$$\mu_{22(310)} = 3V_{2(320)}$$

$$\mu_{22(400)} = V_{2(410)}$$

$$\mu_{33(000)} = V_{3(001)} + \frac{l_\gamma^2}{4} V_{3(003)} + \left(\frac{l_\gamma}{2}\right)^4 V_{3(005)}$$

$$\mu_{33(002)} = 5V_{3(003)} + 5\left(\frac{l_\gamma}{2}\right)^2 V_{3(005)}$$

$$\mu_{33(011)} = 3V_{3(012)} + 3\left(\frac{l_\gamma}{2}\right)^2 V_{3(014)}$$

$$\mu_{33(020)} = V_{3(021)} + \left(\frac{l_\gamma}{2}\right)^2 V_{3(023)}$$

$$\mu_{33(101)} = 3V_{3(102)} + 3\left(\frac{l_\gamma}{2}\right)^2 V_{3(104)}$$

$$\mu_{33(110)} = V_{3(111)} + \left(\frac{l_\gamma}{2}\right)^2 V_{3(113)}$$

$$\mu_{33(200)} = V_{3(201)} + \left(\frac{l_\gamma}{2}\right)^2 V_{3(203)}$$

$$\mu_{33(004)} = 9V_{3(005)}$$

$$\mu_{33(013)} = 7V_{3(014)}$$

$$\mu_{33(022)} = 5V_{3(023)}$$

$$\mu_{33(031)} = 3V_{3(032)}$$

$$\mu_{33(040)} = V_{3(041)}$$

$$\mu_{33(103)} = 7V_{3(104)}$$

$$\mu_{33(112)} = 5V_{3(113)}$$

$$\mu_{33(121)} = 3V_{3(122)}$$

$$\mu_{33(130)} = V_{3(131)}$$

$$\mu_{33(202)} = 5V_{3(203)}$$

$$\mu_{33(211)} = 3V_{3(212)}$$

$$\mu_{33(220)} = V_{3(221)}$$

$$\mu_{33(301)} = 3V_{3(302)}$$

$$\mu_{33(310)} = V_{3(311)}$$

$$\mu_{33(400)} = V_{3(401)}$$

$$\mu_{23(000)} = \frac{1}{2}\left(V_{2(001)} + \left(\frac{l_\gamma}{2}\right)^2 V_{2(003)} + \left(\frac{l_\gamma}{2}\right)^4 V_{2(005)} + V_{3(010)} + \left(\frac{h_\beta}{2}\right)^2 V_{3(030)} + \left(\frac{h_\beta}{2}\right)^4 V_{3(050)}\right)$$

$$\mu_{23(002)} = \frac{1}{2}\left(5V_{2(003)} + 5\left(\frac{l_\gamma}{2}\right)^2 V_{2(005)} + V_{3(012)} + \left(\frac{h_\beta}{2}\right)^2 V_{3(032)}\right)$$

$$\mu_{23(011)} = \frac{1}{2}\left(3V_{2(012)} + 3\left(\frac{l_\gamma}{2}\right)^2 V_{2(014)} + 3V_{3(021)} + 3\left(\frac{h_\beta}{2}\right)^2 V_{3(041)}\right)$$

$$\mu_{23(020)} = \frac{1}{2}\left(V_{2(021)} + \left(\frac{l_\gamma}{2}\right)^2 V_{2(023)} + 5V_{3(030)} + 5\left(\frac{h_\beta}{2}\right)^2 V_{3(050)}\right)$$

$$\mu_{23(101)} = \frac{1}{2}\left(3V_{2(102)} + 3\left(\frac{l_\gamma}{2}\right)^2 V_{2(104)} + V_{3(111)} + \left(\frac{h_\beta}{2}\right)^2 V_{3(131)}\right)$$

$$\mu_{23(110)} = \frac{1}{2}\left(V_{2(111)} + \left(\frac{l_\gamma}{2}\right)^2 V_{2(113)} + 3V_{3(120)} + 3\left(\frac{h_\beta}{2}\right)^2 V_{3(140)}\right)$$

$$\mu_{23(200)} = \frac{1}{2}\left(V_{2(201)} + \left(\frac{l_\gamma}{2}\right)^2 V_{2(203)} + V_{3(210)} + \left(\frac{h_\beta}{2}\right)^2 V_{3(230)}\right)$$

$$\mu_{23(004)} = \tfrac{1}{2}(9V_{2(005)} + V_{3(014)})$$

$$\mu_{23(013)} = \tfrac{1}{2}(7V_{2(014)} + 3V_{3(023)})$$

$$\mu_{23(022)} = \tfrac{1}{2}(5V_{2(023)} + 5V_{3(032)})$$

$$\mu_{23(031)} = \tfrac{1}{2}(3V_{2(032)} + 7V_{3(041)})$$

$$\mu_{23(040)} = \tfrac{1}{2}(V_{2(041)} + 9V_{3(050)})$$

$$\mu_{23(103)} = \tfrac{1}{2}(7V_{2(104)} + V_{3(113)})$$

$$\mu_{23(112)} = \tfrac{1}{2}(5V_{2(113)} + 3V_{3(122)})$$

$$\mu_{23(121)} = \tfrac{1}{2}(3V_{2(122)} + 5V_{3(131)})$$

$$\mu_{23(130)} = \tfrac{1}{2}(V_{2(131)} + 7V_{3(140)})$$

$$\mu_{23(202)} = \tfrac{1}{2}(5V_{2(203)} + V_{3(212)})$$

$$\mu_{23(211)} = \tfrac{1}{2}(3V_{2(212)} + 3V_{3(221)})$$

$$\mu_{23(220)} = \tfrac{1}{2}(V_{2(221)} + 5V_{3(230)})$$

$$\mu_{23(301)} = \tfrac{1}{2}(3V_{2(302)} + V_{3(311)})$$

$$\mu_{23(310)} = \tfrac{1}{2}(V_{2(311)} + 3V_{2(320)})$$

$$\mu_{23(400)} = \tfrac{1}{2}(V_{2(401)} + V_{3(410)})$$

$$\mu_{13(000)} = \frac{1}{2}\left(V_{1(001)} + \left(\frac{l_\gamma}{2}\right)^2 V_{1(003)} + \left(\frac{l_\gamma}{2}\right)^2 V_{1(005)} + V_{3(100)} + \left(\frac{d_\alpha}{2}\right)^2 V_{3(300)} + \left(\frac{d_\alpha}{2}\right)^4 V_{3(500)}\right)$$

$$\mu_{13(002)} = \frac{1}{2}\left(5V_{1(003)} + 5\left(\frac{l_\gamma}{2}\right)^2 V_{1(005)} + V_{3(102)} + \left(\frac{d_\alpha}{2}\right)^2 V_{3(302)}\right)$$

$$\mu_{13(011)} = \frac{1}{2}\left(3V_{1(012)} + 3\left(\frac{l_\gamma}{2}\right)^2 V_{1(014)} + V_{3(111)} + \left(\frac{d_\alpha}{2}\right)^2 V_{3(311)}\right)$$

$$\mu_{13(020)} = \frac{1}{2}\left(V_{1(021)} + \left(\frac{l_\gamma}{2}\right)^2 V_{1(023)} + V_{3(120)} + \left(\frac{d_\alpha}{2}\right)^2 V_{3(320)}\right)$$

$$\mu_{13(101)} = \frac{1}{2}\left(3V_{1(102)} + 3\left(\frac{l_\gamma}{2}\right)^2 V_{1(104)} + 3V_{3(201)} + 3\left(\frac{d_\alpha}{2}\right)^2 V_{3(401)}\right)$$

$$\mu_{13(110)} = \frac{1}{2}\left(V_{1(111)} + \left(\frac{l_\gamma}{2}\right)^2 V_{1(113)} + 3V_{3(210)} + 3\left(\frac{d_\alpha}{2}\right)^2 V_{3(410)}\right)$$

$$\mu_{13(200)} = \frac{1}{2}\left(V_{1(201)} + \left(\frac{l_\gamma}{2}\right)^2 V_{1(203)} + 5V_{3(300)} + 5\left(\frac{d_\alpha}{2}\right)^2 V_{3(500)}\right)$$

$$\mu_{13(004)} = \tfrac{1}{2}(9V_{1(005)} + V_{3(104)})$$

$$\mu_{13(013)} = \tfrac{1}{2}(7V_{1(014)} + V_{3(113)})$$

$$\mu_{13(022)} = \tfrac{1}{2}(5V_{1(023)} + V_{3(122)})$$

$$\mu_{13(031)} = \tfrac{1}{2}(3V_{1(032)} + V_{3(131)})$$

$$\mu_{13(040)} = \tfrac{1}{2}(V_{1(041)} + V_{3(140)})$$

$$\mu_{13(103)} = \tfrac{1}{2}(7V_{1(104)} + 3V_{3(203)})$$

$$\mu_{13(112)} = \tfrac{1}{2}(5V_{1(113)} + 3V_{3(212)})$$

$$\mu_{13(121)} = \tfrac{1}{2}(3V_{1(122)} + 3V_{3(221)})$$

$$\mu_{13(130)} = \tfrac{1}{2}(V_{1(131)} + 3V_{3(230)})$$

$$\mu_{13(202)} = \tfrac{1}{2}(5V_{1(203)} + 5V_{3(302)})$$

$$\mu_{13(211)} = \tfrac{1}{2}(3V_{1(212)} + 5V_{3(311)})$$

$$\mu_{13(220)} = \tfrac{1}{2}(V_{1(221)} + 5V_{3(320)})$$

$$\mu_{13(301)} = \tfrac{1}{2}(3V_{1(302)} + 7V_{3(401)})$$

$$\mu_{13(310)} = \tfrac{1}{2}(V_{1(311)} + 7V_{3(410)})$$

$$\mu_{13(400)} = \tfrac{1}{2}(V_{1(401)} + 9V_{3(500)})$$

$$\mu_{12(000)} = \frac{1}{2}\left(V_{1(010)} + \left(\frac{h_\beta}{2}\right)^2 V_{1(030)} + \left(\frac{h_\beta}{2}\right)^4 V_{1(050)} + V_{2(100)} + \left(\frac{d_\alpha}{2}\right)^2 V_{2(300)} + \left(\frac{d_\alpha}{2}\right)^4 V_{2(500)}\right)$$

$$\mu_{12(002)} = \frac{1}{2}\left(V_{1(012)} + \left(\frac{h_\beta}{2}\right)^2 V_{1(032)} + V_{2(102)} + \left(\frac{d_\alpha}{2}\right)^2 V_{2(302)}\right)$$

$$\mu_{12(011)} = \frac{1}{2}\left(3V_{1(021)} + 3\left(\frac{h_\beta}{2}\right)^2 V_{1(041)} + V_{2(111)} + \left(\frac{d_\alpha}{2}\right)^2 V_{2(311)}\right)$$

$$\mu_{12(020)} = \frac{1}{2}\left(5V_{1(030)} + 5\left(\frac{h_\beta}{2}\right)^2 V_{1(050)} + V_{2(120)} + \left(\frac{d_\alpha}{2}\right)^2 V_{2(320)}\right)$$

$$\mu_{12(101)} = \frac{1}{2}\left(V_{1(111)} + \left(\frac{h_\beta}{2}\right)^2 V_{1(131)} + 3V_{2(201)} + 3\left(\frac{d_\alpha}{2}\right)^2 V_{2(401)}\right)$$

$$\mu_{12(110)} = \frac{1}{2}\left(3V_{1(120)} + 3\left(\frac{h_\beta}{2}\right)^2 V_{1(140)} + 3V_{2(210)} + 3\left(\frac{d_\alpha}{2}\right)^2 V_{2(410)}\right)$$

$$\mu_{12(200)} = \frac{1}{2}\left(V_{1(210)} + \left(\frac{h_\beta}{2}\right)^2 V_{1(230)} + 5V_{2(300)} + 5\left(\frac{d_\alpha}{2}\right)^2 V_{2(500)}\right)$$

$$\mu_{12(004)} = \tfrac{1}{2}(V_{1(014)} + V_{2(104)})$$

$$\mu_{12(013)} = \tfrac{1}{2}(3V_{1(023)} + V_{2(113)})$$

$$\mu_{12(022)} = \tfrac{1}{2}(5V_{1(032)} + V_{2(122)})$$

$$\mu_{12(031)} = \tfrac{1}{2}(7V_{1(041)} + V_{2(131)})$$

$$\mu_{12(040)} = \tfrac{1}{2}(9V_{1(050)} + V_{2(140)})$$

$$\mu_{12(103)} = \tfrac{1}{2}(V_{1(113)} + 3V_{2(203)})$$

$$\mu_{12(112)} = \tfrac{1}{2}(3V_{1(122)} + 3V_{2(212)})$$

$$\mu_{12(121)} = \tfrac{1}{2}(5V_{1(131)} + 3V_{2(221)})$$

$$\mu_{12(130)} = \tfrac{1}{2}(7V_{1(140)} + 3V_{2(230)})$$

$$\mu_{12(202)} = \tfrac{1}{2}(V_{1(212)} + 5V_{2(302)})$$

$$\mu_{12(211)} = \tfrac{1}{2}(3V_{1(221)} + 5V_{2(311)})$$

$$\mu_{12(220)} = \tfrac{1}{2}(5V_{1(230)} + 5V_{2(320)})$$

$$\mu_{12(301)} = \tfrac{1}{2}(V_{1(311)} + 7V_{2(401)})$$

$$\mu_{12(310)} = \tfrac{1}{2}(3V_{1(320)} + 7V_{2(410)})$$

$$\mu_{12(400)} = \tfrac{1}{2}(V_{1(410)} + 9V_{2(500)})$$

The appropriate forms for the Legendre polynomials up through fifth order are

$$P_{(0)} = 1$$

$$P_{(1)} = x$$

$$P_{(2)} = \frac{1}{2}\left(3x^2 - \frac{d^2}{4}\right)$$

$$P_{(3)} = \frac{1}{2}\left(5x^3 - 3\frac{d^2}{4}x\right)$$

$$P_{(4)} = \frac{1}{8}\left(35x^4 - 30\frac{d^2}{4}x^2 + 3\frac{d^4}{16}\right)$$

$$P_{(5)} = \frac{1}{8}\left(63x^5 - 70\frac{d^2}{4}x^3 + 15\frac{d^4}{16}x\right)$$

where d is the subcell dimension along a given direction.

References

Aboudi, J., 1991. Mechanics of Composite Materials: A Unified Micromechanics Approach. Elsevier, New York, NY.
Aboudi, J., 1996. Micromechanical analysis of composites by the method of cells-update. Appl. Mech. Rev. 49, 127–139.
Aboudi, J., Pindera, M.-J., Arnold, S.M., 2001. Linear thermo-elastic higher-order theory for periodic multiphase materials. J. Appl. Mech. 68, 697–707.

Banks-Sills, L., Leiderman, V., Fang, D., 1997. On the effect of particle shape and orientation on elastic properties of metal matrix composites. Comp. B: Eng. 28B, 465–481.

Bensoussan, A., Lions, J.-L., Papanicolaou, G., 1978. Asymptotic Analysis for Periodic Structures. North-Holland, New York, NY.

Benveniste, Y., 1987. A new approach to the application of mori-tanaka's theory in composite materials. Mech. Mater. 6, 147–157.

Christensen, R.M., 1979. Mechanics of Composite Materials. Wiley and Sons, New York, NY.

Eshelby, J.D., 1957. The determination of the elastic field of an ellipsoidal inclusion, and related problems. Proc. Roy. Soc. Lond. A A241, 376–396.

Gilat, R., 1998. On the variational consistency of the higher-order-shear- deformation plate equations derived from the3-d differential equations of motion. Comp. Struct. 41, 285–287.

Hill, R., 1963. Elastic properties of reinforced solids: some theoretical principles. J. Mech. Phys. Solids 11, 357–372.

Nemat-Nasser, S., Hori, M., 1993. Micromechanics: Overall Properties of Heterogeneous Materials. North-Holland, New York, NY.

Paley, M., Aboudi, J., 1992. Micromechanical analysis of composites by the generalized method of cells. Mech. Mater. 14, 127–139.

Soldatos, K.P., 1995. Generalization of variationally consistent plate theories on the basis of a vectorial formulation. J. Sound Vib. 183, 819–839.

Walker, K.P., Freed, A.D., Jordan, E.H., 1993. Accuracy of the generalized self-consistent method in modelling the elastic behavior of periodic composites. Phil. Trans. R. Soc. Lond. A 45, 545–576.

Williams, T.O., Pindera, M.J., 1995. Thermo-mechanical fatigue modeling of advanced metal matrix composites in the presence of microstructural details. Mater. Sci. Eng. A 200, 156–172.

Williams, T.O., Pindera, M.J., 1997. An analytical model for the inelastic longitudinal shear response of metal matrix composites. Int. J. Plasticity 13, 261–289.

Williams, T.O., Aboudi, J., 1999. A generalized micromechanics model with shear-coupling. Acta Mech. 138, 131–154.

Williams, T.O., 2004. A two-dimensional, higher-order, elasticity-based micromechanics model.